

UCSF

UC San Francisco Previously Published Works

Title

Novel Techniques in Imaging Congenital Heart Disease: JACC Scientific Statement.

Permalink

<https://escholarship.org/uc/item/2j7443gm>

Journal

Journal of the American College of Cardiology, 83(1)

Authors

Sachdeva, Ritu

Armstrong, Aimee

Arnaout, Rima

et al.

Publication Date

2024-01-02

DOI

10.1016/j.jacc.2023.10.025

Peer reviewed



HHS Public Access

Author manuscript

J Am Coll Cardiol. Author manuscript; available in PMC 2024 July 02.

Published in final edited form as:

J Am Coll Cardiol. 2024 January 02; 83(1): 63–81. doi:10.1016/j.jacc.2023.10.025.

Novel Techniques in Imaging Congenital Heart Disease:

JACC Scientific Statement

Ritu Sachdeva, MBBS^a, Aimee K. Armstrong, MD^b, Rima Arnaout, MD^c, Lars Grosse-Wortmann, MD^d, B. Kelly Han, MD^e, Luc Mertens, MD, PHD^f, Ryan A. Moore, MD, MSC^g, Laura J. Olivieri, MD^h, Anitha Parthiban, MBBSⁱ, Andrew J. Powell, MD^{j,k}

^aDepartment of Pediatrics, Division of Pediatric Cardiology, Emory University School of Medicine and Children's Healthcare of Atlanta, Atlanta, Georgia, USA

^bThe Heart Center, Nationwide Children's Hospital, Department of Pediatrics, Division of Cardiology, Ohio State University, Columbus, Ohio, USA

^cDivision of Cardiology, Department of Medicine, University of California-San Francisco, San Francisco, California, USA

^dDivision of Cardiology, Department of Pediatrics, Oregon Health and Science University, Portland, Oregon, USA

^eDivision of Cardiology, Department of Pediatrics, University of Utah School of Medicine, Salt Lake City, Utah, USA

^fDivision of Cardiology, Department of Pediatrics, University of Toronto and The Hospital for Sick Children, Toronto, Ontario, Canada

^gThe Heart Institute, Cincinnati Children's Hospital Medical Center, Cincinnati, Ohio, USA

^hDivision of Cardiology, Department of Pediatrics, Children's Hospital of Pittsburgh, Pittsburgh, Pennsylvania, USA

ⁱDepartment of Cardiology, Texas Children's Hospital, Baylor College of Medicine, Houston, Texas, USA

^jDepartment of Cardiology, Boston Children's Hospital, Boston, Massachusetts, USA

^kDepartment of Pediatrics, Harvard Medical School, Boston, Massachusetts, USA

Abstract

Recent years have witnessed exponential growth in cardiac imaging technologies, allowing better visualization of complex cardiac anatomy and improved assessment of physiology. These advances have become increasingly important as more complex surgical and catheter-based procedures are evolving to address the needs of a growing congenital heart disease population.

ADDRESS FOR CORRESPONDENCE: Dr Ritu Sachdeva, Emory University School of Medicine and Children's Healthcare of Atlanta, 1405 Clifton Road, Atlanta, Georgia 30322, USA. sachdevar@kidsheart.com. @RituSachdevaMD.

The authors attest they are in compliance with human studies committees and animal welfare regulations of the authors' institutions and Food and Drug Administration guidelines, including patient consent where appropriate. For more information, visit the Author Center.

APPENDIX For supplemental videos, please see the online version of this paper.

This state-of-the-art review presents advances in echocardiography, cardiac magnetic resonance, cardiac computed tomography, invasive angiography, 3-dimensional modeling, and digital twin technology. The paper also highlights the integration of artificial intelligence with imaging technology. While some techniques are in their infancy and need further refinement, others have found their way into clinical workflow at well-resourced centers. Studies to evaluate the clinical value and cost-effectiveness of these techniques are needed. For techniques that enhance the value of care for congenital heart disease patients, resources will need to be allocated for education and training to promote widespread implementation.

Keywords

angiography; artificial intelligence; cardiac computed tomography; cardiac magnetic resonance; digital twin technology; echocardiography

Cardiac imaging plays a critical role in the diagnosis, treatment, and surveillance of congenital heart disease (CHD). The introduction and dissemination of cutting-edge multimodality imaging techniques can be instrumental in understanding structure and function in complex CHD. Furthermore, advanced imaging enables periprocedural planning for surgical and catheter-based interventions and improves patient outcomes. Although improvements in medical imaging have leveraged rules-based algorithms for decades, the addition of artificial intelligence (AI) algorithms (ie, algorithms that can learn patterns from training data) can increase the speed and flexibility of handling complex imaging data. Use of AI has grown across the imaging modalities and all stages of the imaging pipeline, including patient selection and protocoling, image acquisition, signal denoising, image registration and rendering, quantification, and interpretation (Central Illustration).¹

This *JACC* Scientific Statement provides a comprehensive overview of recent advances in echocardiography, cardiac magnetic resonance imaging (CMR), cardiac computed tomography (CCT), invasive angiography, 3-dimensional (3D) visualization, and digital twin technology for CHD. While some of these novel techniques have been integrated with clinical workflow, others are still in the research phase. A summary of current clinical validation and outcome benefits is provided in Table 1.

ECHOCARDIOGRAPHY

3-DIMENSIONAL ECHOCARDIOGRAPHY.

Recently published consensus guidelines emphasize the high value of 3D echocardiography (3DE) in the evaluation of CHD for valvular disease, complex septal defects, outflow tract obstruction, and abnormalities of intracardiac connections.² As such, 3DE is being increasingly used for surgical planning, real-time guidance of interventions, and quantification of ventricular volumes and function. Applying 3DE to infants and children has required development of high-frequency (6–7 MHz) pediatric transthoracic transducers with smaller footprints. 3D-capable pediatric transducers for transesophageal echocardiography are now available for patients as small as 5 kg. In addition to 3D visualization, the multiplane imaging feature is valuable for rapid assessment in the

operating room. Initial experience has shown safety, feasibility, and quality of 3DE and 2-dimensional (2D) echocardiographic acquisitions.³ Multibeam stitched acquisitions with breath holds are typically needed for adequate resolution, given the high heart rates in children. Recent advances in 3DE acquisition include the ability to obtain and rapidly crop high-quality images from single-beat 3D volume data sets, thus circumventing respiratory and cardiac gating-related artifacts, as well as the ability to manipulate multiplanar images in real time for quantification, especially for catheter guidance procedures.

The structural configuration in CHD can be widely variable, making it difficult to identify important anatomic landmarks and follow them through the course of the imaging study. Novel image rendering technologies can assist in these tasks. Transillumination rendering is a tool that involves manipulation of a virtual light source in 3 dimensions to highlight structures of interest and create shadows to enhance depth perception and improve details compared with traditional rendering (Figures 1 and 2, Videos 1 and 2).⁴ This technique is particularly useful to better delineate orifices and borders for measurement of septal defects and valve areas, and for assessment of valve morphology, commissures, and thin structures such as valve chordae.⁴ Tissue-transparent display options can further highlight the blood-pool tissue interface, and together these rendering options can increase diagnostic value for identification and location of chordal rupture and leaflet clefts as well as for transcatheter edge-to-edge valve repairs compared with standard 3DE.⁵⁻⁸ The addition of color Doppler in the tissue transparency mode allows for accurate definition of regurgitant jets and visualization of flow through orifices and tissues. The ability to place anatomic markers on key structures and simultaneous displays from various perspectives minimizes the need for user manipulation and the risk of erroneous identification of structures.

ULTRAFAST ULTRASOUND.

Traditional ultrasound-based image construction is based on line-per-line focused beam transmissions that have a limited temporal resolution, ranging from 30 to 150 frames per second in current equipment. Ultrafast ultrasound imaging uses unfocused plane-wave ultrasound technology that results in a very high temporal resolution compared with traditional ultrasound. The challenge of lower spatial resolution is addressed by using multiple plane waves for 1 image transmitted at slightly different angles, a technique called coherent compounding. Ultrafast ultrasound results in extremely high frame rates (up to 10,000 frames per second) and allows visualization of very short-lived events, resulting in novel ultrasound applications for studying myocardial and arterial mechanical properties, as well as more sophisticated blood flow imaging techniques for assessing intracavitary flows, myocardial perfusion, and neonatal brain perfusion. These techniques are still largely experimental and under clinical translation, but they have the potential to add significant physiologic information in patients with CHD in the following domains.⁹

Ventricular and vascular function.

Ultrafast ultrasound allows the study of myocardial shear-wave propagation velocities. Myocardial stiffness can then be assessed through the relationship between shear-wave velocity and tissue viscoelastic properties (Young's modulus): the stiffer the tissue, the faster the shear-wave velocity. Different shear-wave imaging techniques have been proposed using

either natural shear waves associated with cardiac mechanical events such as valve closure or externally generated shear waves using acoustic radiation force (Figure 3). Natural shear waves occur at specific time intervals in the cardiac cycle, including at the time of aortic and mitral valve closure. These occur at the interface between systole and diastole and are not true end-systolic or end-diastolic events from a physiologic perspective. The advantage is that they naturally occur and do not depend on externally generated shear waves by the ultrasound probe. Different studies in adults have explored the use of natural shear-wave imaging in both healthy control subjects and patients with different diseases. Most of the work in children has so far been performed using acoustic radiation force, which allows exact timing of the shear wave at end-systole or end-diastole. Initial data reported changes in myocardial stiffness with age¹⁰ and abnormal changes in myocardial stiffness in children with hypertrophic cardiomyopathy.¹¹ Theoretically, end-systolic stiffness should be a load-independent parameter of systolic function and needs to be further explored. Similar ultrafast technology can be applied to vascular imaging to study regional pulse-wave velocities and provides information on regional vascular stiffness.¹² Research on the use of shear-wave imaging in children with acquired heart disease and CHD is currently ongoing. The data files generated by ultrafast ultrasound are very large, requiring large storage capacity and extensive offline processing.

Myocardial and brain perfusion.

Ultrafast ultrasound Doppler applications have also been developed to study blood flow. By applying spatiotemporal clutter filters, coronary ultrafast Doppler angiography allows visualization of the epicardial and intramural coronary microvasculature and quantification of myocardial blood flow. This technique has been optimized for children with the first clinical translation in pediatric cardiac surgery patients.¹³ Similar technology has been applied to image and quantify both global and regional brain perfusion in children undergoing cardiopulmonary bypass surgery in hopes of linking perfusion changes to outcomes in the future.¹⁴

Blood speckle tracking for intracardiac hemodynamics flow assessment.

Whereas conventional color Doppler techniques have been extremely valuable for imaging intracardiac flow direction and velocities, blood speckle tracking combines ultrafast ultrasound imaging with speckle tracking technology to visualize intracardiac and intravascular 2D and 3D flow patterns. This commercially available methodology has been validated for children with CHD and quantifies 2D intracardiac flow velocities, vorticity, and energy losses.¹⁵ The first normal values on vorticity have been published,¹⁶ and initial clinical studies demonstrated changes in flow patterns in children with pulmonary hypertension and after tetralogy of Fallot repair.¹⁷ Blood speckle tracking data can be used for estimating intraventricular pressure differences in children during early diastolic filling, representing early diastolic suction.¹⁸ Further development of quantification techniques based on speckle tracking technology will provide tools to assess how congenital heart defects influence flow patterns as well as cardiac and vascular remodeling.

CARDIAC MAGNETIC RESONANCE IMAGING

HIGHER-DIMENSIONAL FUNCTIONAL IMAGING.

CMR cine imaging and phase-contrast flow velocity mapping are the reference standards for ventricular volumetry and for blood flow quantification, respectively. Traditionally, images are acquired in 2D, 1 to 3 slices at a time, typically during repeated breath holds, which may be challenging for some patients and lead to misalignment of consecutive slices. More recently, a third spatial dimension has been added to these techniques, referred to as 3D or sometimes 4-dimensional (4D) cine (Figure 4, Video 3) and 4D phase contrast (with time as the 4th dimension) so that the images encompass a wide block of anatomy. The principal advantages of this approach include the option to reconstruct the data set in any imaging plane offline and the simplified acquisition planning. Volumetrics derived from 3D CMR are compatible with measures from the traditional 2D approach.¹⁹ Furthermore, automated segmentation of the right ventricle (RV) and left ventricle (LV) from 3D cine data sets, with minimal active reader involvement, may become reality.²⁰ A 4D flow acquisition provides velocity information in all 3 orthogonal planes over the entire cardiac cycle. Velocity maps can be created offline in any user-defined plane, and this obviates the need for precise scan plane prescriptions during the examination. Velocity information can be displayed as stream lines that indicate the orientation of blood flow velocities at a single point in time or path lines that display the spatial trajectory of blood over time. In addition to blood flow volume quantification, 4D flow provides information on advanced hemodynamic measures, such as vorticity, helicity, wall shear stress, kinetic energy loss, pressure gradients, and pulse-wave velocity. It is increasingly used in aortopathies to better understand the relationship between aortic valve morphology and ascending aortic enlargement.²¹ In complex CHD, 4D flow excels at depicting streaming and multilevel shunt quantification (Figure 5, Video 4). Within the cardiac chambers, it quantifies intracavitary blood flow kinetic energy, depicts vortices, and provides insights into atrioventricular valve inflow and regurgitation (Figure 6, Video 5).^{22,23} 3D cine and 4D flow images can be synchronized and displayed in the same 3D data set.¹⁹ Highly accelerated pulse sequences and k-space filling techniques have made 4D flow applicable to routine clinical scans. Sequences that are capable of capturing 2 or more different velocities allow measurements in veins with slower flows and stenotic arteries with faster flows from the same acquisition.²⁴

Most contemporary 3D and 4D functional imaging approaches rely on intravenous contrast agents, such as gadolinium or ferumoxytol, to increase the contrast-to-noise ratio of blood vessels and cardiac chambers. In pediatric applications, it is preferable to minimize intravenous contrast administration to avoid the discomfort of intravenous line placement and potential cumulative effects of contrast administration over a lifetime. However, the lack of contrast along with the aggressive undersampling of k-space needed to keep the scan time within acceptable limits may lead to suboptimal image quality and a low signal-to-noise ratio. AI techniques may address this concern by applying supervised or unsupervised denoising algorithms to accelerate image acquisition and enhance image quality.^{25,26}

MYOCARDIAL TISSUE CHARACTERIZATION.

CMR tissue characterization provides noninvasive assessments of myocardial fibrosis, edema, and iron deposition and is increasingly applied for risk stratification and to determine the timing of reintervention in repaired defects. Myocardial native T1 times and extracellular volume (ECV), derived from pre- and post-contrast T1 times as well as hematocrit, have been used as markers for diffuse fibrosis. T1 parametric mapping has unveiled a number of pathomechanisms of fibrosis, including increased ventricular volume²⁷ or pressure loading,²⁸ cardiopulmonary bypass,²⁹ chronic hypoxia,³⁰ neurohormonal activation, and a genetic disposition.³¹ In tetralogy of Fallot, prolonged T1 times or expanded ECV are associated with decreased myocardial contractility³² and an increased risk for ventricular arrhythmias, hospital admission, or death.³³ In single-ventricle heart disease, they are linked to a composite endpoint of hospital admission, reintervention, Fontan failure, and arrhythmias.³⁴ In patients with Ebstein's anomaly, elevated T1 time is associated with abnormal strain and exercise intolerance.³⁰ Despite these associations, treatment decisions cannot be based on T1 times and ECV in isolation, owing to the significant overlap between myocardial health and disease. Serial measurements have shown promise in understanding a patient's trajectory concerning myocardial fibrotic remodeling.³⁵ Longitudinal outcomes are largely missing but are needed to understand how parametric mapping can inform clinical care. Other tissue markers, such as T2-signal decay times, can be helpful in determining whether an inflammatory component, leading to edema and subsequent T2 prolongation, is present. Together with late gadolinium enhancement, T1 and T2 parametric mapping have been used as a virtual myocardial biopsy with diagnostic value in suspected myocarditis^{36,37} and during organ rejection after heart transplantation.³⁸ More recently, information on T1 and T2 times has been combined into a single sequence, an approach dubbed magnetic resonance fingerprinting.³⁹ In addition to shortening scan time compared with separate T1 and T2 mapping, it provides information on tissue perfusion, diffusion,⁴⁰ fat fraction,⁴¹ T2*, and ECV without the administration of exogenous contrast agents.⁴²

MAGNETIC RESONANCE LYMPHANGIOGRAPHY.

Over the past several years, magnetic resonance (MR) has yielded unique insights into the anatomy and physiology of the lymphatic system⁴³ and has largely replaced diagnostic fluoroscopic lymphangiography in the CHD population. Static MR lymphangiography approaches rely on high-resolution T2-weighted sequences, often combined with 3D steady-state free precession acquisitions for visualization of thoracic duct anatomy and landmark structures.⁴⁴ Unlike static T2-weighted imaging, dynamic contrast-enhanced magnetic resonance lymphangiography (DCMRL) provides information on the direction of chylous flow by tracking the passage of gadolinium-based contrast through the circulation with sequential T1-weighted imaging.^{45,46} Contrast is injected via a groin lymph node or, less commonly, the periportal lymph passages or a mesenteric lymph node, and imaged repeatedly at regular intervals for a total of 7 to 15 minutes. At the end, a high-resolution 3D data set, typically with fat suppression, is acquired for optimal spatial definition. The interpretation of DCMRL images can be challenging, because the simultaneous enhancement of veins may confound the visualization of lymphatic channels. This limitation has been tempered by the dual-agent relaxivity contrast technique in which an intravenous injection of ferumoxytol is followed by DCMRL with a gadolinium-based contrast

agent.⁴⁷ When imaged with an extended-echo mDixon-sequence MR pulse sequence, the ferumoxytol suppresses gadolinium venous enhancement, allowing for isolation of lymphatic channels without venous contamination.

Lymphatic imaging with MR has greatly enhanced our understanding of lymphatic disorders that can complicate CHD, particularly in patients undergoing sequential surgical palliations for single-ventricle heart disease (Figure 7). The elevated central venous pressure in children with Fontan physiology increases lymphatic production and interferes with lymphatic return to the central venous system. The resultant lymphatic engorgement contributes to the development of protein-losing enteropathy, plastic bronchitis, and chylous effusions. A greater lymphatic burden, assessed by T2-weighted imaging, is associated with adverse outcomes after the Fontan operation, including chylous effusions, heart failure, transplant assessment, recurrent effusions, thrombi, and protein losing enteropathy.⁴⁸ Moreover, MR lymphangiography has furthered the opportunities for interventions in the lymphatic system, interrupting or at least slowing the pathophysiology that leads to the above clinical complications.

CARDIAC COMPUTED TOMOGRAPHY

CCT RADIATION DOSE OPTIMIZATION.

Studies indicating increased cancer risk related to computed tomographic (CT) scans in children reinforce that dose optimization is critical for patient safety. In addition, patients with CHD have an increased intrinsic risk of malignancy, bolstering the “as low as reasonably achievable” principle for CT scans in CHD.⁴⁹ In response to this critical need, there have been multiple recent developments over the past few years to reduce radiation dose. Standard techniques for electrocardiography-gated scans now include using prospective gating when possible, limiting radiation dose to a narrow acquisition window, using the lowest tube voltage and current for each patient and indication, and limiting cine imaging (Figure 8). Dose reductions of 85%–90% have been shown in CHD patients with the use of these measures and operator education.^{50,51} AI algorithms may further assist by improving image reconstruction from low-dose CT imaging.⁵²

Functional or cine CCT is increasingly used for assessment of valve anatomy before percutaneous intervention and to quantify ventricular size and function in CHD patients with implanted devices affecting CMR safety or image quality. Cine CCT imaging requires radiation throughout the cardiac cycle. Electrocardiography-gated pulse modulation allows definition of a narrow “full-dose” window in the cardiac cycle and the delivery of minimal radiation (eg, 20% of the full dose) for the rest of the cardiac cycle. Automated tube-current modulation determines the scanner output providing the lowest dose to the patient while maintaining user-defined reference image quality. Noise level is maintained constant throughout the scan range by automatically varying tube current along the z-axis of the patient based on monitoring sequences. Further radiation dose reduction is possible with the use of increasingly sophisticated image processing tools that decrease noise in the reconstructed data sets after acquisition. Model-based iterative reconstruction and deep learning algorithms using neural networks trained on high-quality data sets may allow significant prospective reduction in radiation dose without negatively affecting

image quality, based on phantom data and preliminary data in CHD patients.⁵³ These advances in radiation dose reduction with maintained excellent image quality will further minimize diagnostic risk and allow expanded use of CCT in CHD patients with appropriate indications.

PHOTON-COUNTING CT.

Traditional CT scanners convert x-rays to visible light, which is then converted into an electronic signal providing analog image data. Limitations of this approach include averaging of the x-ray signal leading to a monoenergetic image reconstruction, susceptibility to electronic noise, and a ceiling on the achievable spatial resolution. Photon-counting detectors are newer technology that overcome these drawbacks by converting the x-ray signal directly into an electronic signal without the intervening conversion to light. Individual photon energy is measured directly and weighted independently, which allows low-energy photons to be differentiated from electronic noise. The data acquired from different-energy photons increases the contrast-to-noise ratio and provides spectral information in all scans without the need for dual-energy scanning or rapid kVp switching. There is potential for multiple energy reconstructions from the same scan data, including a virtual noncontrast scan, calcium maps, iodine maps, measurement of extracellular volume, and coronary plaque quantification.⁵⁴ The decrease in image noise reduces the impact of calcium and metallic artifact on image quality, and sharper reconstruction kernels can be used. Because there is no need for separation between detector elements, spatial resolution is improved, with a baseline resolution of 0.4 mm and ultra-high spatial resolution of 0.2 mm at the scan isocenter. Reports on the clinical use of photon-counting scanners have primarily come from studies in phantoms, adult cardiac imaging, and noncardiac pediatric imaging.^{55,56} Photon-counting CCT data in children with CHD is beginning to emerge,⁵⁷ and it should become clear in the next few years whether the promise of improved resolution, lower radiation doses, and novel applications come to fruition.

CORONARY ARTERY FRACTIONAL FLOW RESERVE.

Fractional flow reserve (FFR) assesses the physiologic effect of coronary artery obstruction to determine the utility of intervention in intermediate lesions. Invasive FFR uses a guidewire in the coronary artery to measure the pressure drop distal to a lesion under conditions of maximal hyperemia, typically induced with intracoronary adenosine. The distal coronary pressure is compared with aortic pressure and reported as a ratio. Noninvasive FFR from CT imaging (CT FFR) is a method of measuring FFR with the use of computational fluid dynamics to mathematically model coronary flow, pressure, and resistance based on an individual's 3D coronary and myocardial anatomy. A patient-specific physiologic model is created from the CT data, with the resting myocardial blood flow proportional to the myocardial mass and the microvascular resistance inversely proportional to the size of the epicardial coronary arteries. Several randomized controlled trials have demonstrated good correlation between invasive FFR and CT FFR in adult patients undergoing evaluation of coronary artery disease.⁵⁸

CT FFR may have utility in patients with coronary artery stenosis after reimplantation as part of CHD surgery, those with a history of Kawasaki disease or cardiac transplantation

and coronary artery pathology, and those with anomalous aortic origin of a coronary artery (AAOCA) (Figure 9). A study of the retrospective performance of CT FFR in an adult population with AAOCA did not show a difference in CT FFR for those considered to be at higher risk based on anatomic features vs those considered to be at lower risk in 5-year follow-up.⁵⁹ However, the focus on older patients may select for a benign form of AAOCA, and these findings may not be relevant for pediatric patients. Thus far, prospective CT FFR in AAOCA patients has been described only in case reports.⁶⁰ Although it is appealing to envision CCT providing both anatomic and physiologic assessment, there are several hurdles that must be overcome before adoption into clinical practice. The low rate of adverse events in patients with AAOCA or after surgical coronary reimplantation would hinder investigations of the value of CT FFR to risk-stratify patients and identify those that warrant surgical intervention. Moreover, it is not known whether the flow modeling based on atherosclerotic coronary artery disease would apply to the different anatomic substrate of AAOCA, the smaller coronary arteries of children, aneurysm or serial stenosis in Kawasaki disease, or proximal coronary stenosis after surgical coronary intervention in the setting of CHD. The appropriate stress condition for CT FFR is also unclear. In addition to simulating increased flow, it may be important, for example, to simulate increased aortic pressure and the resulting deformation of the aortic wall and proximal coronary artery.⁶¹ Therefore, further studies are needed to guide the clinical use of CT FFR in pediatric and CHD patients.

INVASIVE ANGIOGRAPHY

3D ROTATIONAL ANGIOGRAPHY.

Three-dimensional rotational angiography (3DRA) creates a volumetric data set of contrast-enhanced CT-like images with excellent visualization of soft tissues and airway and a spatial resolution that is better than with multi-detector CT and CMR.⁶² This is accomplished by the single-plane C-arm flat panel detector rotating around the patient over 4 to 5 seconds during contrast injection. The image information collected provides a 2D angiogram with 200° to 240° of viewing, a 3D reconstruction that can be manipulated to view the structures from all angles, and a multiplanar reformat. Intraluminal fly-through and clipping-plane views allow an endovascular assessment of stents, aneurysms, vessel wall irregularities, and calcification⁶² (Videos 6 and 7).

When advanced imaging is not performed before catheterization to avoid additional general anesthesia, radiation, or contrast load, 3DRA allows a “1-stop shop” for imaging, diagnosis, treatment, and even 3D printing (3DP).⁶³ By providing a comprehensive view of relationship of cardiac structures, vessels, and the airway, 3DRA overcomes the limitations of 2D angiography. It enhances intervention safety and effectiveness by showing the impact of stents on adjacent structures and elucidating the mechanism of a stenosis. 3DRA takes the guesswork out of gantry angles for 2D angiography by showing the angle that will optimize the image, thereby decreasing the number of 2D angiograms and radiation dose.⁶⁴ Because the 3D reconstruction is in geometric correspondence with the C-arm coordinates, it can be automatically registered and overlaid onto live fluoroscopy to assist with interventions and decrease the number of 2D angiograms (Video 5). In fact, studies have shown that its use provides superior diagnostic quality compared with 2D angiography and improves

procedural efficiency without increasing radiation or contrast load.^{65,66} High-quality 3DRA images have been shown to be significantly associated with greater injection volume, more dilute contrast solution, and lower patient weight, and these data have been used to create a novel 3DRA nomogram for estimating the probability of a high-quality 3DRA.⁶⁷

While 3DRA has the capability of bringing personalized medicine to the congenital catheterization laboratory, there are several areas for future advancement. First, using 3DRA imaging and the hemodynamics from diagnostic catheterization, computational fluid dynamics (CFD) can be performed with virtual stenting so that the operator can predict the postintervention hemodynamic outcome before doing the intervention. Feasibility of this technique has been shown in patients with coarctation.⁶⁸ Incorporating machine learning can enhance computational speed for complete hemodynamic assessment and virtual interventions.⁶⁹ Second, moving from time-averaged to time-resolved 4DRA would allow systolic dimensions to be obtained for interventional planning and would provide functional analysis, ventricular volumetrics, and 4D flow. Third, 3DRA overlay on live fluoroscopy needs to compensate for cardiac and respiratory motion such that the 3D image moves with the live fluoroscopy, and early work with fully automated software is promising.⁷⁰ Automatic correction should also be developed to update the overlaid model to account for vascular deformity caused by stiff wires and long sheaths during the procedure.⁷¹ AI has already been used to improve the registration and automatic correction process of overlaying on live fluoroscopy.⁷² Finally, 3DRA needs to move to biplane acquisition with the use of 2 detectors to improve workflow and decrease contrast load.

FUSION IMAGING.

3D reconstructions from echocardiography, CMR, CCT, and 3DRA can be fused with fluoroscopy for real-time procedural guidance.⁷³⁻⁷⁵ For fusion to be useful, it is imperative that the overlaid images are properly registered with the fluoroscopy. This technique has been shown to reduce radiation exposure with excellent safety and usability in children.⁷⁶

INTERVENTIONAL CMR IMAGING.

X-ray fluoroscopy lacks soft tissue imaging and real-time visualization, whereas CMR offers superior soft tissue imaging and dynamic views without radiation. Catheterization with CMR would be ideal, but challenges such as radiofrequency-induced heating, limited visibility of standard catheters, and metallic artifacts obstructing imaging have hindered interventional CMR (ICMR). The desire to avoid radiation-related health risks and musculoskeletal injuries from lead protection has driven efforts to overcome these limitations.

ICMR was initially used in pediatric patients on a large scale to perform right heart catheterization.⁷⁷ As the field has progressed, specific equipment has been developed for catheterization, including an MR-conditional guidewire with passive MR markers. It has been successfully used in patients with CHD to perform right or left heart catheterization, to measure pressure gradients across stenoses with MR guidance⁷⁸ and to test occluded Fontan fenestrations.⁷⁹

The field of ICMR has been slow to develop in large part because of the lack of MR-conditional equipment visible by MR. The lack of research and development for MR equipment, however, is largely due to the few numbers of users. This circular problem may be broken by low-field (eg, 0.55-T) scanners, which may allow the use of commercially available catheterization equipment, because radiofrequency-induced heating of interventional devices is reduced at low field strength (theoretical 7.5-fold difference in heating between 0.55-T and 1.5-T).⁸⁰ Preclinical testing of inferior vena cava stenting with the use of real-time low-field MR imaging (0.55-T) in a large animal model showed excellent visualization of commercially available 316L stainless steel stent implantations on angioplasty balloons with proprietary MR-visible markers (Figure 10).⁸¹ Marking of conventional catheters and interventional equipment with passive markers is 1 technique that will move the field forward by increasing available devices. If low field is to be used for ICMR in the future, however, cardiovascular imaging must be optimized under the conditions of low signal-to-noise ratio and limited gradient performance. Fortunately, preclinical and clinical testing has demonstrated that a comprehensive CMR protocol is feasible on an 80-cm ultrawide-bore commercial 0.55-T MR system, including compressed-sensing 2D phase-contrast cine, dynamic contrast-enhanced imaging for myocardial perfusion, 3D MR angiography, and tissue characterization with the use of late gadolinium enhancement.⁸²

3D VISUALIZATION, 3D MEDICAL MODELING, AND DIGITAL TWIN TECHNOLOGY

3D VISUALIZATIONS AND ANATOMIC DIGITAL TWINS.

Three-dimensional visualization of cardiac anatomy is now an important element in diagnostic imaging and procedural planning for CHD. Over the past 10 years, 3D reconstructions have taken on many new derivatives beyond a single 2D display, including: 1) 3DP; 2) extended realities (XR); and 3) holographic imaging.^{83–86} Significant advances in 3D cardiac imaging have driven 3D visualization techniques to more interactive solutions, including virtual procedural planning (VPP), CFD, and fusion imaging (Figure 11). These novel tools provide imaging guidance, both offline and real-time, to enhance clinical decision making and improve outcomes.

As health care and digital technology continue to converge, there is a precedent to align with current terminology to facilitate communication between industry and medicine. In many industries, digital twins are virtual models of a physical object that are often used to simulate the object's behavior, predict outcomes, and optimize performance. For this reason, we propose using the term “anatomic digital twin” in place of “patient-specific 3D model” for imaging reconstructions.⁸⁷

IMAGE SEGMENTATION AND 3D MEDICAL MODELING.

Creation of anatomic digital twins typically begins with imaging segmentation, a binary process of sorting voxels (ie, the 3D analogs of pixels) of data from source images to be either included or excluded from the 3D model. Segmentation methods vary significantly, from the application of a simple source imaging threshold to semiautomatic and machine

learning-driven methods, which can predict and create complex shapes found in CHD by means of multiple layers of segmentation.⁸⁸ Segmentation requires 3D medical modeling software that can both: 1) display DICOM images with proper alignment and spatial information; and 2) create, modify, and codify segmentation masks to form a 3D digital model.⁸⁹ There is significant variability in cost, functionality, and usability of segmentation software with options ranging from: 1) coding to create segmentation; to 2) window-like programs that extend the complex segmentation task performance for users without coding experience; and 3) software that allows users to segment in virtual reality (VR) for an immersive experience.⁹⁰ Finally, segmentation can be performed on any 3D imaging data set, including 3DE, CCT, CMR, and 3DRA.⁹¹

Segmented masks can be smoothed, subtracted, and combined to create either blood pool models or intracardiac models that are hollow and mimic myocardial and vessel surface structure; the latter are often favored for surgical planning. From there, these 3D digital model files have multiple digital outputs, including a display of a 3D file on a 2D screen, display of a 3D file in a 3D augmented reality (AR) or VR type format, and display of a 3D file in a tangible, printed manner using 3DP and additive manufacturing techniques.

Finally, 3D visualization technologies typically rely on segmentation to create a model in 3D space, but immersive visualization of 3D imaging data including 3DE and CMR or CCT is also used and discussed separately in this review.

3DP AND 3D BIOPRINTING.

The most universally adopted method for applying 3D anatomic digital twins in pediatric CHD is to print a segmented surface model by means of 3DP.⁹² There are 4 methods of 3DP that are used in health care: 1) fused deposition modeling; 2) selective laser sintering; 3) stereo-lithography; and 4) polyjet printing. These methods vary in construction materials (polymers and metals), model cost (\$10 to \$1,000s), time to print (minutes to hours), and spatial resolution (30–250 μm). Best practices have evolved in 3DP for CHD, and attention must be paid to the quality of the surface segmentation and to the planes where the 3D model will be cut so that inner details will be revealed accurately and effectively. Cut-planes are of particular importance when crafting 3DP models to plan or practice complex procedures; access must be offered to the operator (ie, surgeon or interventionist) that simulates the access they will have during the procedure. Valverde et al published multicenter findings in 2017 demonstrating the value of 3DP heart models in surgical procedural planning.⁹³

Bioprinting is an emerging field wherein biocompatible replacement tissues are manufactured in specific shapes to allow for resorption and cellular seeding once inside the body. Although very promising, there are still considerable regulatory and technologic hurdles before this technology is more widely available for the treatment of CHD.

Many 3D medical laboratories working to create anatomic digital twins are opting to display them digitally owing to the high inherent cost and time of 3DP. However, 3DP is still the technology of choice for several centers to: 1) simulate complex CHD procedures⁹⁴; and 2)

create engineered tissue grafts and other bioprinted materials for implantation of a specific surgical shape and material (eg, surgical guides).

VIRTUAL PROCEDURAL PLANNING.

VPP is defined as the use of an anatomic digital twin for surgical or interventional procedural planning. The current state in which VPP is often referenced is simply 3D visualizations using the latest digital technology tools; however, the ultimate goal is for the proceduralist to be able to fully manipulate an anatomic digital twin in a “sandbox”-like environment to achieve true planning of a procedure. Historically, this VPP took place before the procedure and heavily relied on desktop-based planning⁹⁵; however, recent advances in XR have allowed for translation of these digital technologies into both the preprocedural and intraprocedural settings. XR is an all-encompassing term that includes AR, VR, and mixed reality. Currently, AR and VR are the predominant technologies in the pediatric cardiac planning space. AR describes a rendered image being overlaid onto the real world, and VR is rendered images in a fully immersive virtual environment. Tsai et al⁹⁶ summarize the XR technologies in terms of their positive and significant impact on education, patient/family empowerment, and health care team processes. Stephenson et al⁹⁷ also provide a thorough review of XR technologies in the cardiac space, citing many studies that provide a descriptive use profile of emerging technologies, although few prove direct patient benefit owing to the rapid pace and nature of technology implementation. They also raise the issue of measurement validation with these technologies. There are several XR software solutions currently available or in development, including: 1) pre-existing 3D medical modeling/segmentation software with added XR solutions; 2) new VR software focused on 3D medical modeling/segmentation in an immersive space; 3) game engine-enhanced solutions for creating and operating interactive realtime 3D content; and 4) AR volume-rendered registration systems that overlay virtual and physical landmarks for intraprocedural guidance. Both surface-rendered and volume-rendered digital anatomic twins have been used, with surface meshes being favored for VR-based model manipulation and volume meshes for intraprocedural anatomic overlay.

Catheter-based procedures have started to apply AR/VR techniques mostly for medical device anatomic overlay, such as planning balloon-expandable trans-catheter pulmonary valve placement⁹⁸ and other device or stent-based procedures.⁹⁹ Surgical procedures have started to use AR/VR techniques for: 1) advanced 3D visualizations; 2) medical device anatomic overlay; and 3) interactive manipulation of anatomic digital twins for advanced VPP. 3D visualizations using AR/VR are relatively common in the imaging market and are often used to “plan” operations by enhancing the surgeon’s understanding of intracardiac and extracardiac anatomic relationships, such as for complex biventricular repairs.¹⁰⁰ A step toward more interactive planning includes overlaying medical device digital twins onto anatomic structures in a virtual environment in an effort to better simulate device position and “fit,” as is commonly needed when using adult-sized devices in pediatric or small size patients.^{86,101–103} To achieve universal adoption from more experienced surgeons, there needs to be advancements in VR simulation that allow them to generate actual surgical plans using patient-specific anatomic digital twins vs 3D visualization alone. As such, 3D models used in surgical planning must be situated in a “sandbox” that has minimal restraints on

user interaction with the model and its environment and must integrate virtual correlates of tissue handling that would enhance the realism of the VR planning and its translation to the clinical setting. Early attempts to apply these modalities to virtual surgical planning have shown great promise, but additional work is necessary to push these platforms into routine clinical use.¹⁰⁴ Finally, building a multi-user VR environment for CHD surgical planning that allows for worldwide collaboration between expert surgeons, surgical trainees, 3D imaging specialists, and outcome-centered cardiologists will allow for the type of global impact that this technology promises.

CFD, FINITE ELEMENTAL ANALYSIS, AND OTHER SIMULATIONS.

In addition to virtual and printed displays, these 3D anatomic digital twins can be used to predict hemodynamic performance through application of CFD simulations, which are a step toward 3D physiologic digital twins. By applying generally accepted equations that govern fluid dynamics and deriving boundary conditions of flow, pressure, and resistance from available clinical data (eg, CMR or catheterization), 3D modeling has been used to predict hemodynamic indices based on anatomic shape. This is increasingly used in surgical planning of complex CHD, and studies have shown a correlation between CFD results and exercise capacity and energetics in Fontan,¹⁰⁵ tetralogy of Fallot,¹⁰⁶ and coarctation of the aorta.¹⁰⁷

Current state-of-the-art CFD can incorporate uncertainty into solutions over a range of boundary conditions (eg, flow variations and small anatomic variations) to mimic various physiologic states on the geometry.¹⁰⁸ These methods scale to larger mesh and design spaces but are limited when using unsteady flows. Deep learning together with computational flow simulation is being used to fill these gaps, for example, when modeling aortic flow in normal and disease states and in modeling valve disease.^{109,110} Finally, comprehensive surgical planning software platforms that rely on CFD and anatomic digital twins are in development at multiple sites in order to reduce human effort and turnaround time, and to optimize postoperative hemodynamics.

SUMMARY, GAPS, AND FUTURE DIRECTIONS

This review highlights some of the recent advances in echocardiography, CMR, CCT, invasive angiography, 3D medical modeling, and AI that have had or are expected to have an important impact on the care of patients with CHD. Other developments and modalities will also undoubtedly contribute to this goal. For many of the advances described here, further work is needed to rigorously assess their clinical value and cost-effectiveness. It is crucial that diagnostic imaging care pathways and appropriate use criteria for common scenarios be established to avoid both overuse and underuse of these new technologies. Training and education for both imaging specialists and nonspecialists will be crucial to achieving this aim.

Supplementary Material

Refer to Web version on PubMed Central for supplementary material.

FUNDING SUPPORT AND AUTHOR DISCLOSURES

Dr Armstrong is a consultant for Edwards Lifesciences, Medtronic, Cook Medical, Abbott, and Starlight Cardiovascular; and receives research support from Siemens Healthineers and Renata Medical.

Dr Grosse-Wortmann is a consultant for Siemens Healthineers. Dr Powell is a consultant for Siemens Healthineers. All other authors have reported that they have no relationships relevant to the contents of this paper to disclose.

ABBREVIATIONS AND ACRONYMS

2D	2-dimensional
3D	3-dimensional
3DE	3-dimensional echocardiography
3DP	3-dimensional printing
3DRA	3-dimensional rotational angiography
4D	4-dimensional
AAOCA	anomalous aortic origin of a coronary artery
AI	artificial intelligence
AR	augmented reality
CCT	cardiac computed tomography
CFD	computational fluid dynamics
CHD	congenital heart disease
CMR	cardiac magnetic resonance imaging
CT	computed tomography
DCMRL	dynamic contrast-enhanced magnetic resonance lymphangiography
ECV	extracellular volume
FFR	fractional flow reserve
ICMR	interventional cardiac magnetic resonance
LV	left ventricle
MR	magnetic resonance
RV	right ventricle
VPP	virtual procedural planning
VR	virtual reality
XR	extended realities

REFERENCES

1. Dey D, Arnaout R, Antani S, et al. Proceedings of the NHLBI Workshop on Artificial Intelligence in Cardiovascular Imaging: state-of-the-art review. *J Am Coll Cardiol Img* 2023;16(9):1209–1223.
2. Simpson J, Lopez L, Acar P, et al. Three-dimensional echocardiography in congenital heart disease: an expert consensus document from the European Association of Cardiovascular Imaging and the American Society of Echocardiography. *J Am Soc Echocardiogr* 2017;30(1):1–27. [PubMed: 27838227]
3. Shah SS, A D, Madan N, et al. Initial experience with Pediatric 3D Transesophageal Echo Probe and Imaging System. Abstract presented at: 8th World Congress of Pediatric Cardiology and Cardiac Surgery; August 27–September 1, 2023; Washington, DC.
4. Genovese D, Addetia K, Kebed K, et al. First clinical experience with 3-dimensional echocardiographic transillumination rendering. *J Am Coll Cardiol Img* 2019;12(9):1868–1871.
5. Sun F, Sun A, Chen Y, et al. Novel TrueVue series of 3D echocardiography: revealing the pathological morphology of congenital heart disease. *Front Physiol* 2022;13:1000007. [PubMed: 36148295]
6. Karagodin I, Addetia K, Singh A, et al. Improved delineation of cardiac pathology using a novel three-dimensional echocardiographic tissue transparency tool. *J Am Soc Echocardiogr* 2020;33(11):1316–1323. [PubMed: 32972777]
7. Tamborini G, Mantegazza V, Garlasche A, et al. Head to head comparison between different 3-dimensional echocardiographic rendering tools in the imaging of percutaneous edge-to-edge mitral valve repair. *J Cardiovasc Dev Dis* 2021;8(7).
8. Volpato V, Mantegazza V, Tamborini G, et al. Diagnostic accuracy of transillumination in mitral valve prolapse: side-by-side comparison of standard transthoracic three-dimensional echocardiography against surgical findings. *J Am Soc Echocardiogr* 2021;34(1):98–100. [PubMed: 33036821]
9. Villemain O, Baranger J, Friedberg MK, et al. Ultrafast ultrasound imaging in pediatric and adult cardiology: techniques, applications, and perspectives. *J Am Coll Cardiol Img* 2020;13(8):1771–1791.
10. Malik A, Baranger J, Nguyen MB, et al. Impact of ventricular geometrical characteristics on myocardial stiffness assessment using shear wave velocity in healthy children and young adults. *J Am Soc Echocardiogr* 2023;36(8):849–857. [PubMed: 36842514]
11. Villemain O, Correia M, Khraiche D, et al. Myocardial stiffness assessment using shear wave imaging in pediatric hypertrophic cardiomyopathy. *J Am Coll Cardiol Img* 2018;11(5):779–781.
12. Rasouli R, Baranger J, Slorach C, et al. Local arterial stiffness assessment: comparison of pulse wave velocity assessed by ultrafast ultrasound imaging versus the Bramwell-Hill equation. *J Am Soc Echocardiogr* 2022;35(11):1185–1188. [PubMed: 35863547]
13. Zhang N, Nguyen MB, Mertens L, Barron DJ, Villemain O, Baranger J. Improving coronary ultrafast Doppler angiography using fractional moving blood volume and motion-adaptive ensemble length. *Phys Med Biol* 2022;67(12): 125021.
14. Aguet J, Fakhari N, Nguyen M, et al. Impact of cardiopulmonary bypass on cerebrovascular autoregulation assessed by ultrafast ultrasound imaging. *J Physiol* 2023;601(6):1077–1093. [PubMed: 36779673]
15. Nyrnes SA, Fadnes S, Wigen MS, Mertens L, Lovstakken L. Blood speckle-tracking based on high-frame rate ultrasound imaging in pediatric cardiology. *J Am Soc Echocardiogr* 2020;33(4): 493–503.e495. [PubMed: 31987749]
16. Marchese P, Cantinotti M, Van den Eynde J, et al. Left ventricular vortex analysis by high-frame rate blood speckle tracking echocardiography in healthy children and in congenital heart disease. *Int J Cardiol Heart Vasc* 2021;37:100897. [PubMed: 34786451]
17. Mawad W, Lovstakken L, Fadnes S, et al. Right ventricular flow dynamics in dilated right ventricles: energy loss estimation based on blood speckle tracking echocardiograph—a pilot study in children. *Ultrasound Med Biol* 2021;47(6):1514–1527. [PubMed: 33685744]

18. Sørensen K, Fadnes S, Mertens L, et al. Assessment of early diastolic intraventricular pressure difference in children by blood speckle-tracking echocardiography. *J Am Soc Echocardiogr* 2023;36(5):523–532.e3. [PubMed: 36632939]
19. Moghari MH, van der Geest RJ, Brighenti M, Powell AJ. Cardiac magnetic resonance using fused 3D cine and 4D flow sequences: validation of ventricular and blood flow measurements. *Magn Reson Imaging* 2020;74:203–212. [PubMed: 33035637]
20. Van der Ven JPG, van Genuchten W, Sadighy Z, et al. Multivendor evaluation of automated MRI postprocessing of biventricular size and function for children with and without congenital heart defects. *J Magn Reson Imaging* 2023;58(3):794–804. [PubMed: 36573004]
21. Johnson EMI, Scott MB, Jarvis K, et al. Global aortic pulse wave velocity is unchanged in bicuspid aortopathy with normal valve function but elevated in patients with aortic valve stenosis: insights from a 4D Flow MRI study of 597 subjects. *J Magn Reson Imaging* 2023;57(1):126–136. [PubMed: 35633284]
22. Kaur H, Assadi H, Alabed S, et al. Left ventricular blood flow kinetic energy assessment by 4D flow cardiovascular magnetic resonance: a systematic review of the clinical relevance. *J Cardiovasc Dev Dis* 2020;7(3):37. [PubMed: 32927744]
23. Gorecka M, Bissell MM, Higgins DM, Garg P, Plein S, Greenwood JP. Rationale and clinical applications of 4D flow cardiovascular magnetic resonance in assessment of valvular heart disease: a comprehensive review. *J Cardiovasc Magn Reson* 2022;24(1):49. [PubMed: 35989320]
24. Ma LE, Markl M, Chow K, Vali A, Wu C, Schnell S. Efficient triple-VENC phase-contrast MRI for improved velocity dynamic range. *Magn Reson Med* 2020;83(2):505–520. [PubMed: 31423646]
25. Jung W, Lee HS, Seo M, et al. MR-self Noise2Noise: self-supervised deep learning-based image quality improvement of submillimeter resolution 3D MR images. *Eur Radiol* 2023;33(4): 2686–2698. [PubMed: 36378250]
26. Xia Y, Ravikumar N, Greenwood JP, Neubauer S, Petersen SE, Frangi AF. Super-resolution of cardiac MR cine imaging using conditional GANs and unsupervised transfer learning. *Med Image Anal* 2021;71:102037. [PubMed: 33910110]
27. Yim D, Riesenkampff E, Caro-Dominguez P, Yoo SJ, Seed M, Grosse-Wortmann L. Assessment of diffuse ventricular myocardial fibrosis using native T1 in children with repaired tetralogy of Fallot. *Circ Cardiovasc Imaging* 2017;10(3): e005695. [PubMed: 28292861]
28. Dusenbery SM, Lunze FI, Jerosch-Herold M, et al. Left ventricular strain and myocardial fibrosis in congenital aortic stenosis. *Am J Cardiol* 2015;116(8):1257–1262. [PubMed: 26343231]
29. Riesenkampff E, Luining W, Seed M, et al. Increased left ventricular myocardial extracellular volume is associated with longer cardiopulmonary bypass times, biventricular enlargement and reduced exercise tolerance in children after repair of tetralogy of Fallot. *J Cardiovasc Magn Reson* 2016;18(1):75. [PubMed: 27782857]
30. Aly S, Seed M, Yoo SJ, Lam C, Grosse-Wortmann L. Myocardial fibrosis in pediatric patients with Ebstein's anomaly. *Circ Cardiovasc Imaging* 2021;14(3):e011136. [PubMed: 33722068]
31. Vaikom House AK, Chetan D, Mital S, Grosse-Wortmann L. Patients with repaired tetralogy of Fallot and the HIF1A1744C/T variant have increased imaging markers of diffuse myocardial fibrosis. *Int J Cardiol* 2022;350:33–35. [PubMed: 34973973]
32. de Alba CG, Khan A, Woods P, Broberg CS. Left ventricular strain and fibrosis in adults with repaired tetralogy of Fallot: a case-control study. *Int J Cardiol* 2021;323:34–39. [PubMed: 32882293]
33. Broberg CS, Chugh SS, Conklin C, Sahn DJ, Jerosch-Herold M. Quantification of diffuse myocardial fibrosis and its association with myocardial dysfunction in congenital heart disease. *Circ Cardiovasc Imaging* 2010;3(6):727–734. [PubMed: 20855860]
34. Pisesky A, Reichert MJE, de Lange C, et al. Adverse fibrosis remodeling and aortopulmonary collateral flow are associated with poor Fontan outcomes. *J Cardiovasc Magn Reson* 2021;23(1):134. [PubMed: 34781968]
35. Karur GR, Mawad W, Grosse-Wortmann L. Progressive right ventricular outflow tract fibrosis after repair of tetralogy of Fallot. *Cardiol Young* 2020;30(9):1366–1367. [PubMed: 32718363]

36. Cornicelli MD, Rigsby CK, Rychlik K, Pahl E, Robinson JD. Diagnostic performance of cardiovascular magnetic resonance native T1 and T2 mapping in pediatric patients with acute myocarditis. *J Cardiovasc Magn Reson* 2019;21(1):40. [PubMed: 31307467]
37. Law YM, Lal AK, Chen S, et al. Diagnosis and management of myocarditis in children: a scientific statement from the American Heart Association. *Circulation* 2021;144(6):e123–135. [PubMed: 34229446]
38. Soslow JH, Samyn MM. Multi-modal imaging of the pediatric heart transplant recipient. *Transl Pediatr* 2019;8(4):322–338. [PubMed: 31728325]
39. Liu Y, Hamilton J, Rajagopalan S, Seiberlich N. Cardiac magnetic resonance fingerprinting: technical overview and initial results. *J Am Coll Cardiol Img* 2018;11(12):1837–1853.
40. Ma D, Gulani V, Seiberlich N, et al. Magnetic resonance fingerprinting. *Nature* 2013;495(7440):187–192. [PubMed: 23486058]
41. Ostenson J, Damon BM, Welch EB. MR fingerprinting with simultaneous T1, T2, and fat signal fraction estimation with integrated B₀ correction reduces bias in water T₁ and T₂ estimates. *Magn Reson Imaging* 2019;60:7–19. [PubMed: 30910696]
42. Wang CY, Coppo S, Mehta BB, Seiberlich N, Yu X, Griswold MA. Magnetic resonance fingerprinting with quadratic RF phase for measurement of T₂* simultaneously with d_f, T₁, and T₂. *Magn Reson Med* 2019;81(3):1849–1862. [PubMed: 30499221]
43. Chavhan GB, Lam CZ, Greer MC, Temple M, Amaral J, Grosse-Wortmann L. Magnetic resonance lymphangiography. *Radiol Clin North Am* 2020;58(4):693–706. [PubMed: 32471538]
44. Gooty VD, Veeram Reddy SR, Greer JS, et al. Lymphatic pathway evaluation in congenital heart disease using 3D whole-heart balanced steady state free precession and T2-weighted cardiovascular magnetic resonance. *J Cardiovasc Magn Reson* 2021;23(1):16. [PubMed: 33641664]
45. Ramirez-Suarez KI, Tierradentro-Garcia LO, Smith CL, et al. Dynamic contrast-enhanced magnetic resonance lymphangiography. *Pediatr Radiol* 2022;52(2):285–294. [PubMed: 33830292]
46. Chavhan GB, Amaral JG, Temple M, Itkin M. MR Lymphangiography in children: technique and potential applications. *Radiographics* 2017;37(6):1775–1790. [PubMed: 29019760]
47. Maki JH, Neligan PC, Briller N, Mitsumori LM, Wilson GJ. Dark blood magnetic resonance lymphangiography using dual-agent relaxivity contrast (DARC-MRL): a novel method combining gadolinium and iron contrast agents. *Curr Probl Diagn Radiol* 2016;45(3):174–179. [PubMed: 26460054]
48. Ghosh RM, Griffis HM, Glatz AC, et al. Prevalence and cause of early fontan complications: does the lymphatic circulation play a role? *J Am Heart Assoc* 2020;9(7):e015318. [PubMed: 32223393]
49. Lupo PJ, Schraw JM, Desrosiers TA, et al. Association between birth defects and cancer risk among children and adolescents in a population-based assessment of 10 million live births. *JAMA Oncol* 2019;5(8):1150–1158. [PubMed: 31219523]
50. Meinel FG, Henzler T, Schoepf UJ, et al. ECG-synchronized CT angiography in 324 consecutive pediatric patients: spectrum of indications and trends in radiation dose. *Pediatr Cardiol* 2015;36(3):569–578. [PubMed: 25380963]
51. Ali F, Rizvi A, Ahmad H, et al. Quality initiative to reduce cardiac CT angiography radiation exposure in patients with congenital heart disease. *Pediatr Qual Saf* 2019;4(3):e168. [PubMed: 31579868]
52. Greffier J, Si-Mohamed S, Frandon J, et al. Impact of an artificial intelligence deep-learning reconstruction algorithm for CT on image quality and potential dose reduction: a phantom study. *Med Phys* 2022;49(8):5052–5063. [PubMed: 35696272]
53. Hee Kim K, Choo KS, Jin Nam K, et al. Cardiac CTA image quality of adaptive statistical iterative reconstruction-V versus deep learning reconstruction “TrueFidelity” in children with congenital heart disease. *Medicine (Baltimore)* 2022;101(42): e31169. [PubMed: 36281124]
54. Kim NY, Im DJ, Youn JC, et al. Synthetic extracellular volume fraction derived using virtual unenhanced attenuation of blood on contrast-enhanced cardiac dual-energy CT in nonischemic cardiomyopathy. *AJR Am J Roentgenol* 2022;218(3):454–461. [PubMed: 34643105]

55. Tsiflikas I, Thater G, Ayx I, et al. Low dose pediatric chest computed tomography on a photon counting detector system—initial clinical experience. *Pediatr Radiol* 2023;53(6):1057–1062. [PubMed: 36635378]
56. Cao J, Bache S, Schwartz FR, Frush D. Pediatric applications of photon-counting detector CT. *AJR Am J Roentgenol* 2023:1–10. [PubMed: 36542746]
57. Dirrichs T, Tietz E, Ruffer A, et al. Photon-counting versus dual-source CT of congenital heart defects in neonates and infants: initial experience. *Radiology* 2023;307(5):e223088. [PubMed: 37219443]
58. Ko BS, Cameron JD, Munnur RK, et al. Noninvasive CT-derived FFR based on structural and fluid analysis: a comparison with invasive FFR for detection of functionally significant stenosis. *J Am Coll Cardiol Img* 2017;10(6):663–673.
59. Adjedj J, Hyafil F, Halna du Fretay X, et al. Physiological evaluation of anomalous aortic origin of a coronary artery using computed tomography-derived fractional flow reserve. *J Am Heart Assoc* 2021;10(7):e018593. [PubMed: 33728970]
60. Molossi S, Doan T, Sachdeva S. Anomalous coronary arteries: a state-of-the-art approach. *Cardiol Clin* 2023;41(1):51–69. [PubMed: 36368811]
61. Bigler MR, Stark AW, Giannopoulos AA, et al. Coronary CT FFR vs invasive adenosine and dobutamine FFR in a right anomalous coronary artery. *J Am Coll Cardiol Case Rep* 2022;4(15):929–933.
62. Kang SL, Armstrong A, Krings G, Benson L. Three-dimensional rotational angiography in congenital heart disease: present status and evolving future. *Congenit Heart Dis* 2019;14(6): 1046–1057. [PubMed: 31483574]
63. Seckeler MD, Boe BA, Barber BJ, Berman DP, Armstrong AK. Use of rotational angiography in congenital cardiac catheterisations to generate three-dimensional-printed models. *Cardiol Young* 2021;31(9):1407–1411. [PubMed: 33597057]
64. Minderhoud SCS, Van der Stelt F, Molenschot MMC, Koster MS, Krings GJ, Breur J. Dramatic dose reduction in three-dimensional rotational angiography after implementation of a simple dose reduction protocol. *Pediatr Cardiol* 2018;39(8):1635–1641. [PubMed: 30076424]
65. Stenger A, Dittrich S, Glockler M. Three-dimensional rotational angiography in the pediatric cath lab: optimizing aortic interventions. *Pediatr Cardiol* 2016;37(3):528–536. [PubMed: 26667957]
66. Haddad L, Waller BR, Johnson J, et al. Radiation protocol for three-dimensional rotational angiography to limit procedural radiation exposure in the pediatric cardiac catheterization lab. *Congenit Heart Dis* 2016;11(6):637–646. [PubMed: 27079433]
67. Salavitarab A, Boe BA, Berman DP, et al. Optimizing 3D rotational angiography for congenital cardiac catheterization. *Pediatr Cardiol* 2023;44(1):132–140. [PubMed: 36029321]
68. Armstrong AK, Zampi JD, Itu LM, Benson LN. Use of 3D rotational angiography to perform computational fluid dynamics and virtual interventions in aortic coarctation. *Catheter Cardiovasc Interv* 2020;95(2):294–299. [PubMed: 31609061]
69. Nita CI, Puiu A, Bunescu D, et al. Personalized pre- and post-operative hemodynamic assessment of aortic coarctation from 3D rotational angiography. *Cardiovasc Eng Technol* 2022;13(1):14–40. [PubMed: 34145556]
70. Assink NIM, Nempont O, et al. Feasibility of fully automated motion compensated overlay for transcatheter aortic valve implantation. *J Struct Heart Dis* 2018;4(5):207–211.
71. Smorenburg SPM, Lely RJ, Smit-Ockeloen I, Yeung KK, Hoksbergen AWJ. Automated image fusion during endovascular aneurysm repair: a feasibility and accuracy study. *Int J Comput Assist Radiol Surg* 2023.
72. Bailey CJ, Edwards JB, Giarelli M, Zwiebel B, Grundy L, Shames M. Cloud-based fusion imaging improves operative metrics during fenestrated endovascular aneurysm repair. *J Vasc Surg* 2023;77(2):366–373. [PubMed: 36181994]
73. Jone PN, Haak A, Ross M, et al. Congenital and structural heart disease interventions using echocardiography-fluoroscopy fusion imaging. *J Am Soc Echocardiogr* 2019;32(12):1495–1504. [PubMed: 31597599]

74. Grant EK, Kanter JP, Olivieri LJ, et al. X-ray fused with MRI guidance of pre-selected transcatheter congenital heart disease interventions. *Catheter Cardiovasc Interv* 2019;94(3):399–408. [PubMed: 31062506]
75. Arar Y, Reddy SRV, Kim H, et al. 3D advanced imaging overlay with rapid registration in CHD to reduce radiation and assist cardiac catheterisation interventions. *Cardiol Young* 2020;30(5):656–662. [PubMed: 32290877]
76. Ehret N, Alkassar M, Dittrich S, et al. A new approach of three-dimensional guidance in paediatric cath lab: segmented and tessellated heart models for cardiovascular interventions in CHD. *Cardiol Young* 2018;28(5):661–667. [PubMed: 29345604]
77. Ratnayaka K, Kanter JP, Faranesh AZ, et al. Radiation-free CMR diagnostic heart catheterization in children. *J Cardiovasc Magn Reson* 2017;19(1):65. [PubMed: 28874164]
78. Meierhofer C, Belker K, Shehu N, et al. Real-time CMR guidance for intracardiac and great vessel pressure mapping in patients with congenital heart disease using an MR conditional guidewire—results of 25 patients. *Cardiovasc Diagn Ther* 2021;11(6):1356–1366. [PubMed: 35070804]
79. Veeram Reddy SR, Arar Y, Zahr RA, et al. Invasive cardiovascular magnetic resonance (iCMR) for diagnostic right and left heart catheterization using an MR-conditional guidewire and passive visualization in congenital heart disease. *J Cardiovasc Magn Reson* 2020;22(1):20. [PubMed: 32213193]
80. Campbell-Washburn AE, Ramasawmy R, Restivo MC, et al. Opportunities in interventional and diagnostic imaging by using high-performance low-field-strength MRI. *Radiology* 2019;293(2):384–393. [PubMed: 31573398]
81. Armstrong A, Krishnamurthy R, Swinning J, Liu Y, Joseph M, Simonetti O. Feasibility of MRI-guided cardiac catheterization, angioplasty, and stenting in a 0.55 T scanner with limited gradient performance. *Pediatr Cardiol* 2022;43:1972.
82. Varghese J, Jin N, Giese D, et al. Building a comprehensive cardiovascular magnetic resonance exam on a commercial 0.55 T system: a pictorial essay on potential applications. *Front Cardiovasc Med* 2023;10:1120982. [PubMed: 36937932]
83. Ong CS, Krishnan A, Huang CY, et al. Role of virtual reality in congenital heart disease. *Congenit Heart Dis* 2018;13(3):357–361. [PubMed: 29399969]
84. Raimondi F, Vida V, Godard C, et al. Fast-track virtual reality for cardiac imaging in congenital heart disease. *J Card Surg* 2021;36(7):2598–2602. [PubMed: 33760302]
85. Bruckheimer E, Rotschild C, Dagan T, et al. Computer-generated real-time digital holography: first time use in clinical medical imaging. *Eur Heart J Cardiovasc Imaging* 2016;17(8):845–849. [PubMed: 27283456]
86. Szugye NA, Zafar F, Villa C, Lorts A, Morales DLS, Moore RA. 3D holographic virtual surgical planning for a single right ventricle Fontan patient needing Heartmate III placement. *ASAIO J* 2021;67(12):e211–215. [PubMed: 34261876]
87. Pesapane F, Rotili A, Penco S, Nicosia L, Cassano E. Digital twins in radiology. *J Clin Med* 2022;11(21):6553. [PubMed: 36362781]
88. Giannopoulos AA, Mitsouras D, Yoo SJ, Liu PP, Chatzizisis YS, Rybicki FJ. Applications of 3D printing in cardiovascular diseases. *Nat Rev Cardiol* 2016;13(12):701–718. [PubMed: 27786234]
89. Lasso A, Herz C, Nam H, et al. SlicerHeart: an open-source computing platform for cardiac image analysis and modeling. *Front Cardiovasc Med* 2022;9:886549. [PubMed: 36148054]
90. Sutherland J, Belec J, Sheikh A, et al. Applying modern virtual and augmented reality technologies to medical images and models. *J Digit Imaging* 2019;32(1):38–53. [PubMed: 30215180]
91. Olivieri LJ, Krieger A, Loke YH, Nath DS, Kim PC, Sable CA. Three-dimensional printing of intracardiac defects from three-dimensional echocardiographic images: feasibility and relative accuracy. *J Am Soc Echocardiogr* 2015;28(4):392–397. [PubMed: 25660668]
92. Yoo SJ, Thabit O, Kim EK, et al. 3D printing in medicine of congenital heart diseases. *3D Print Med* 2015;2(1):3. [PubMed: 30050975]
93. Valverde I, Gomez-Ciriza G, Hussain T, et al. Three-dimensional printed models for surgical planning of complex congenital heart defects: an international multicentre study. *Eur J Cardiothorac Surg* 2017;52(6):1139–1148. [PubMed: 28977423]

94. Olivieri L, Krieger A, Chen MY, Kim P, Kanter JP. 3D heart model guides complex stent angioplasty of pulmonary venous baffle obstruction in a Mustard repair of D-TGA. *Int J Cardiol* 2014;172(2):e297–298. [PubMed: 24447757]
95. Moore RA, Riggs KW, Kourtidou S, et al. Three-dimensional printing and virtual surgery for congenital heart procedural planning. *Birth Defects Res* 2018;110(13):1082–1090. [PubMed: 30079634]
96. Tsai TY, Onuma Y, Zlahoda-Huzior A, et al. Merging virtual and physical experiences: extended realities in cardiovascular medicine. *Eur Heart J* 2023;44(35):3311–3322. [PubMed: 37350487]
97. Stephenson N, Pushparajah K, Wheeler G, Deng S, Schnabel JA, Simpson JM. Extended reality for procedural planning and guidance in structural heart disease—a review of the state-of-the-art. *Int J Cardiovasc Imaging* 2023;39(7): 1405–1419. [PubMed: 37103667]
98. Jolley MA, Lasso A, Nam HH, et al. Toward predictive modeling of catheter-based pulmonary valve replacement into native right ventricular outflow tracts. *Catheter Cardiovasc Interv* 2019;93(3):E143–E152. [PubMed: 30444053]
99. Tandon A, Burkhardt BEU, Batsis M, et al. Sinus venosus defects: anatomic variants and transcatheter closure feasibility using virtual reality planning. *J Am Coll Cardiol Img* 2019;12(5): 921–924.
100. Bruning J, Kramer P, Goubergrits L, et al. 3D modeling and printing for complex biventricular repair of double outlet right ventricle. *Front Cardiovasc Med* 2022;9:1024053. [PubMed: 36531701]
101. Moore RA, Lorts A, Madueme PC, Taylor MD, Morales DL. Virtual implantation of the 50cc SynCardia total artificial heart. *J Heart Lung Transplant* 2016;35(6):824–827. [PubMed: 26899766]
102. Moore RA, Madueme PC, Lorts A, Morales DL, Taylor MD. Virtual implantation evaluation of the total artificial heart and compatibility: beyond standard fit criteria. *J Heart Lung Transplant* 2014;33(11):1180–1183. [PubMed: 25239034]
103. Davies RR, Hussain T, Tandon A. Using virtual reality simulated implantation for fit testing pediatric patients for adult ventricular assist devices. *JTCVS Tech* 2021;6:134–137. [PubMed: 34318173]
104. Kim B, Nguyen P, Loke YH, et al. Virtual reality cardiac surgical planning software (CorFix) for designing patient-specific vascular grafts: development and pilot usability study. *JMIR Cardio* 2022;6(1):e35488. [PubMed: 35713940]
105. Mercer-Rosa L, Fogel MA, Wei ZA, et al. Fontan geometry and hemodynamics are associated with quality of life in adolescents and young adults. *Ann Thorac Surg* 2022;114(3):841–847. [PubMed: 35120878]
106. Loke YH, Capuano F, Cleveland V, Mandell JG, Balaras E, Olivieri LJ. Moving beyond size: vorticity and energy loss are correlated with right ventricular dysfunction and exercise intolerance in repaired tetralogy of Fallot. *J Cardiovasc Magn Reson* 2021;23(1):98. [PubMed: 34412634]
107. Mandell JG, Loke YH, Mass PN, et al. Altered hemodynamics by 4D flow cardiovascular magnetic resonance predict exercise intolerance in repaired coarctation of the aorta: an in vitro study. *J Cardiovasc Magn Reson* 2021;23(1):99. [PubMed: 34482836]
108. Contento J, Mass P, Cleveland V, et al. Location matters: offset in tissue-engineered vascular graft implantation location affects wall shear stress in porcine models. *JTCVS Open* 2022;12:355–363. [PubMed: 36590712]
109. Pajaziti E, Montalt-Tordera J, Capelli C, et al. Shape-driven deep neural networks for fast acquisition of aortic 3D pressure and velocity flow fields. *PLoS Comput Biol* 2023;19(4):e1011055. [PubMed: 37093855]
110. Yevtushenko P, Goubergrits L, Franke B, Kuehne T, Schafstedde M. Modelling blood flow in patients with heart valve disease using deep learning: a computationally efficient method to expand diagnostic capabilities in clinical routine. *Front Cardiovasc Med* 2023;10:1136935. [PubMed: 36937926]

HIGHLIGHTS

- Cardiac imaging plays a crucial role in the evaluation and management of patients with congenital heart disease.
- Advancements in cardiac imaging techniques will likely find rapid clinical application in the assessment of patients with congenital heart disease.
- Strategies to assess clinical value and resources for training are needed before widespread implementation.

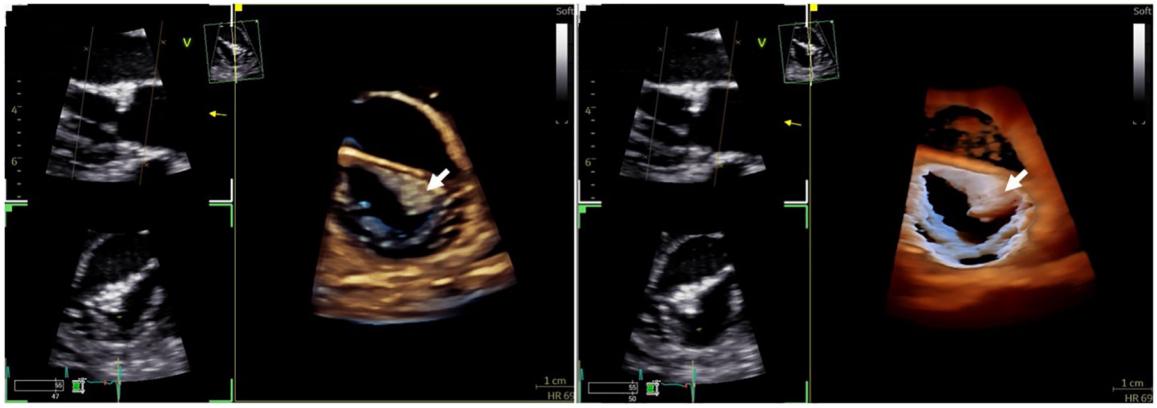


FIGURE 1. 3D Transthoracic Echocardiography of the Mitral Valve With Transillumination
Comparison of 3D echocardiographic rendering of a mass on the mitral valve leaflet (white arrow) with traditional imaging (left) vs transillumination (right), which offers better delineation of borders and depth perception.

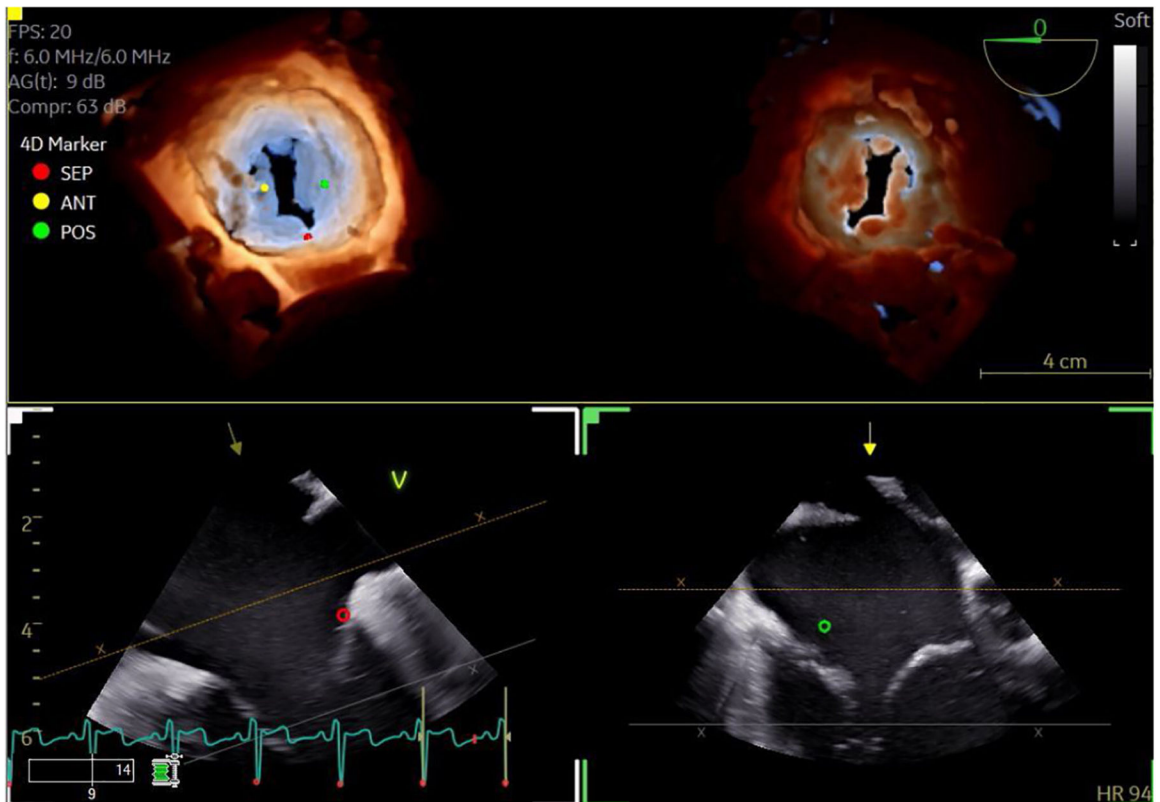


FIGURE 2. 3D Transesophageal Echocardiography of the Tricuspid Valve With Transillumination

3D transesophageal echocardiographic image of the tricuspid valve with transillumination to highlight the leaflet edges and commissures (top left: view from the right atrium; top right: view from the right ventricle). Markers have been placed to indicate the leaflets. Dual crop feature allows for rapid and simultaneous visualization from multiple perspectives.

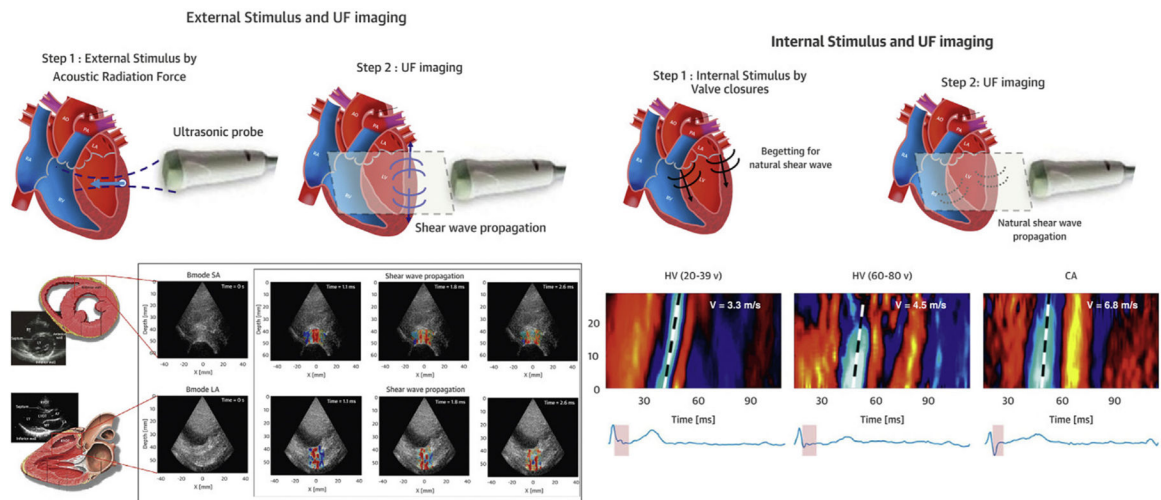


FIGURE 3. Shear-Wave Imaging

(Left) SWI based on acoustic radiation force, which allows exact timing of the shear wave at end-systole or end-diastole. (Right) SWI of natural mechanical waves associated with cardiac mechanical events such as valve closure. CA = cardiac amyloidosis; HV = healthy volunteers; SWI = shear-wave imaging; UF = ultrafast. Adapted from Tamborini et al⁷ with permission.

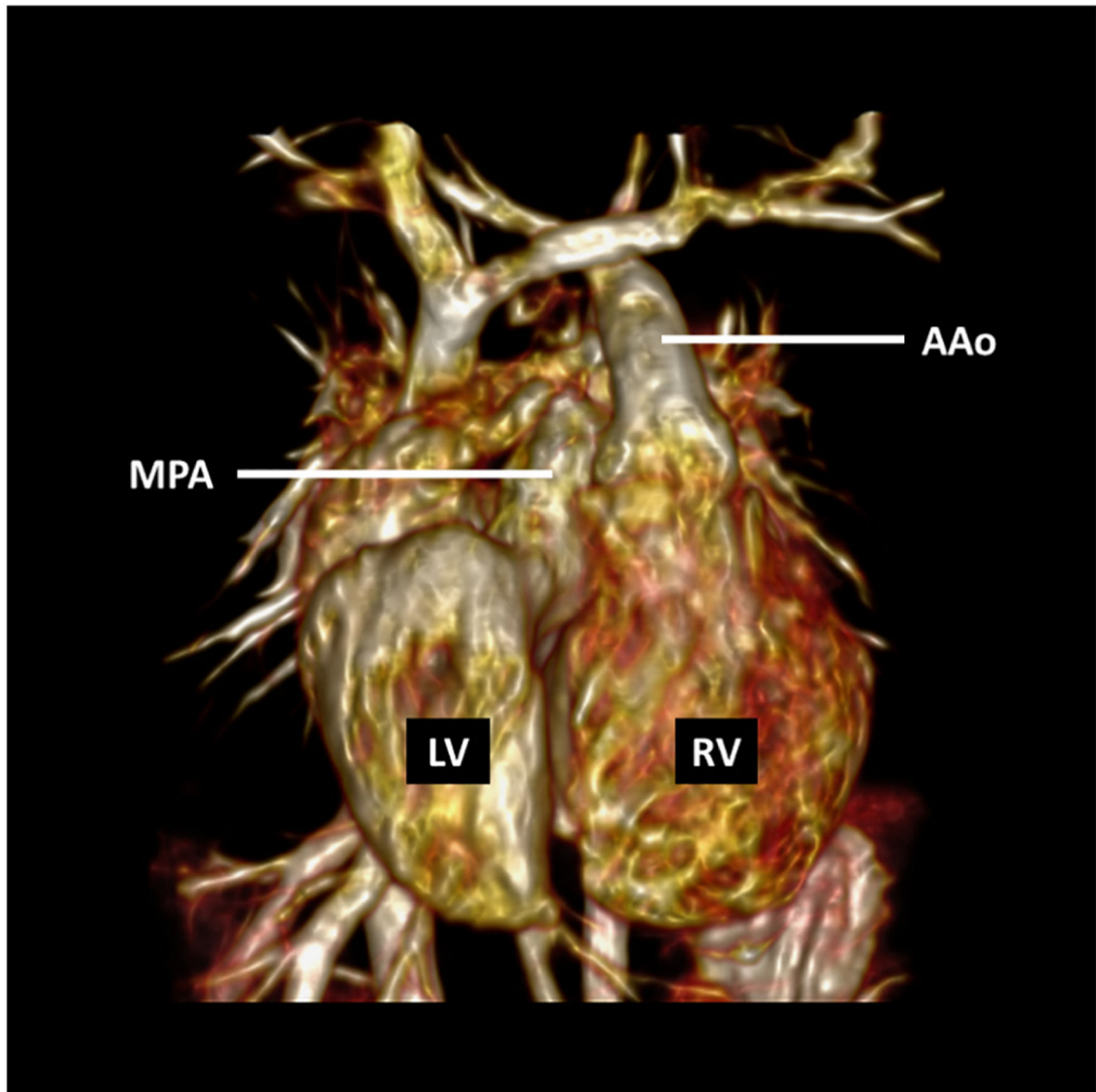


FIGURE 4. 3D Cine Magnetic Resonance Imaging

Steady-state free precession sequence with a temporal resolution of 20 phases per cardiac cycle obtained after administration of a gadolinium-based contrast agent in a 2-year-old girl with mesocardia, congenitally corrected transposition of the great arteries, and ventricular septal defect who underwent surgical pulmonary artery band placement. AAo = ascending aorta; LV = left ventricle; MPA = main pulmonary artery; RV = right ventricle.

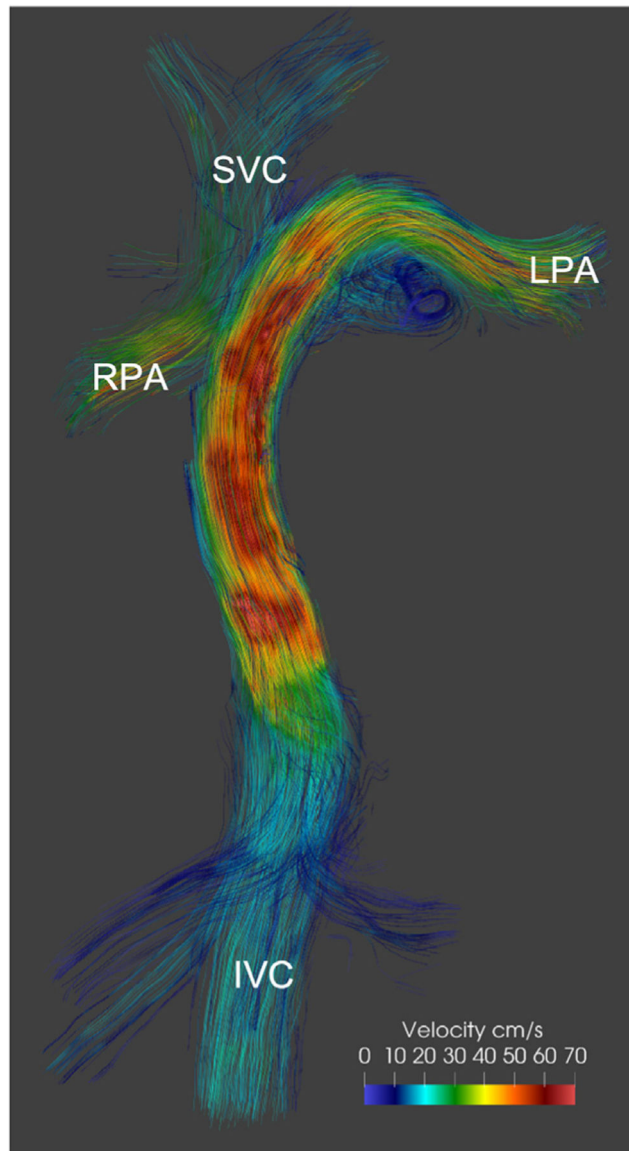


FIGURE 5. Vascular 4D Flow

The 4D phase contrast acquisition in a patient after the Fontan procedure demonstrates preferential blood flow from the inferior vena cava (IVC) to the left pulmonary artery (LPA) and from the superior vena cava (SVC) to the right pulmonary artery (RPA). Image provided by F. Rijnberg, Leiden, the Netherlands.

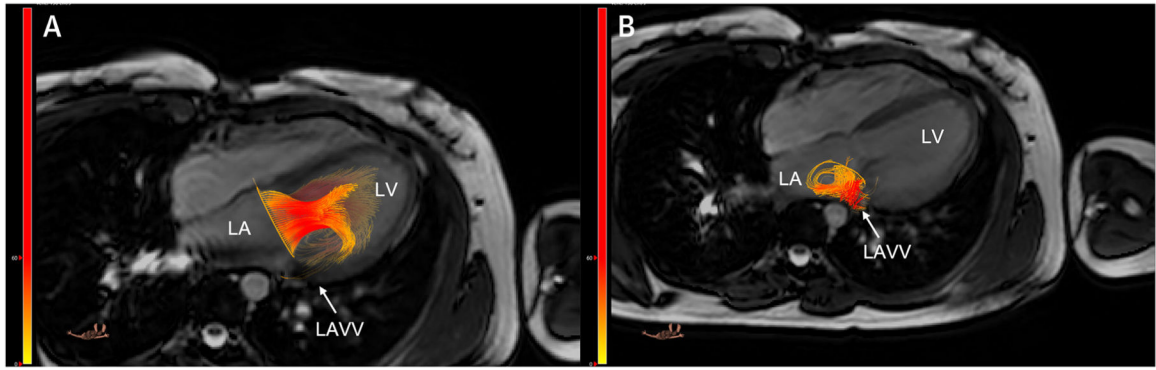


FIGURE 6. Intracardiac 4D Flow

A 4D flow study with retrospective tracking of the valve plane in a patient after repair of an atrioventricular septal defect demonstrates left atrioventricular valve (A) inflow and (B) regurgitation. LA = left atrium; LAVV = left atrioventricular valve; LV = left ventricle. Images provided by J. Westenberg, Leiden, the Netherlands.

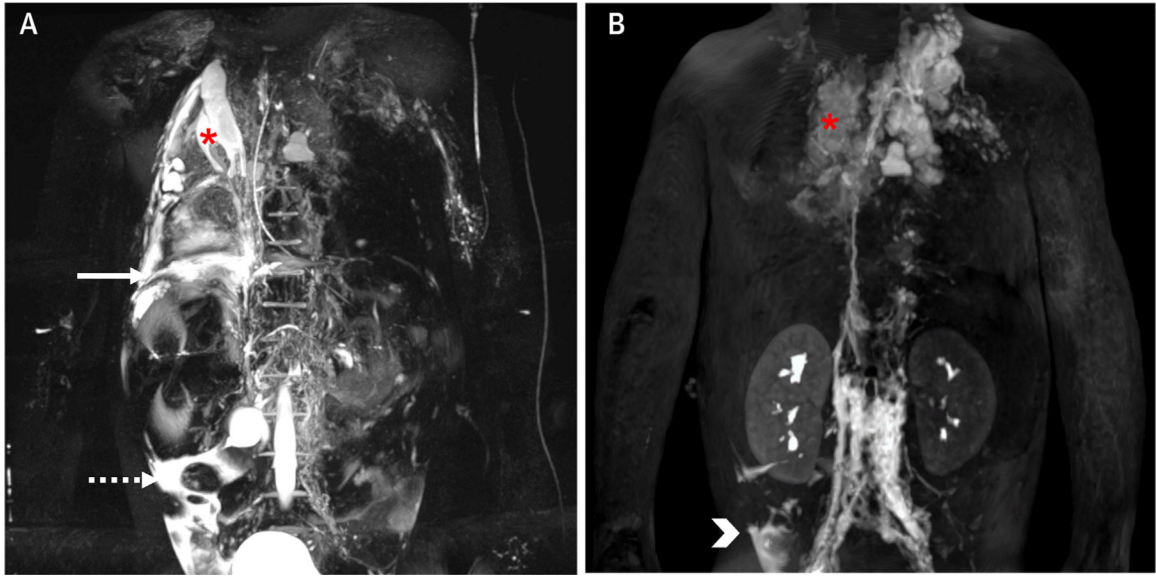


FIGURE 7. Magnetic Resonance Lymphangiography

(A) 3D T2-weighted turbo spin echo acquisition and (B) still frame from a 3D T1-weighted sequence 14 minutes after injection during a dynamic contrast-enhanced magnetic resonance lymphangiography (DCMRL) acquisition in a 4-year-old patient with failing Fontan, plastic bronchitis, and chronic chylous effusions. The static T2-weighted images show severely abnormal thoracic lymphatics with right pulmonary lymphangiectasia (asterisk), as well as a right-side pleural effusion (solid arrow) and ascites (dashed arrow). The DCMRL shows retrograde lymphatic flow to both lungs, especially to the right (asterisk), as well as a subhepatic peritoneal lymphatic leak (arrowhead). Images provided by C. Lam, Toronto, Canada.

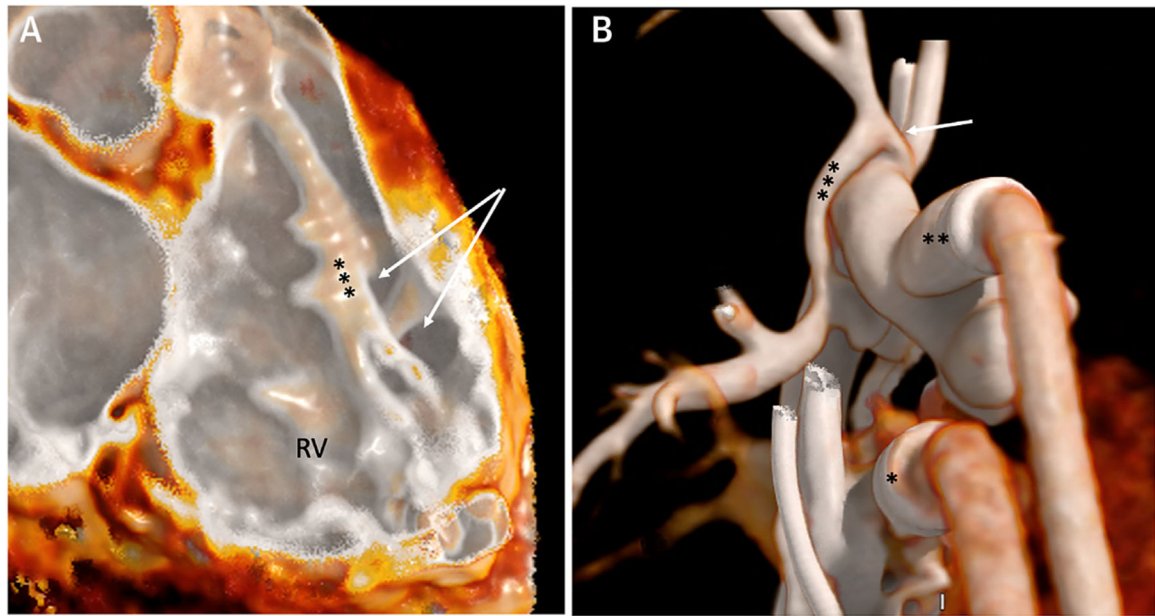


FIGURE 8. CCT Images With the Use of Low Radiation

Electrocardiography-gated CCT images using single heart beat with low radiation. (A) Intraluminal view of the right ventricle (RV) showing a muscular ventricular septal defect (arrows) posterior to the septomarginal trabeculation (***). (B) External 3D reconstruction of venous (*) and arterial (**) ventricular assist device cannula in a patient with single-ventricle congenital heart disease. Narrowing of the innominate artery (arrow) is noted proximal to the systemic-to-pulmonary artery shunt (***) insertion. CCT = cardiac computed tomography.

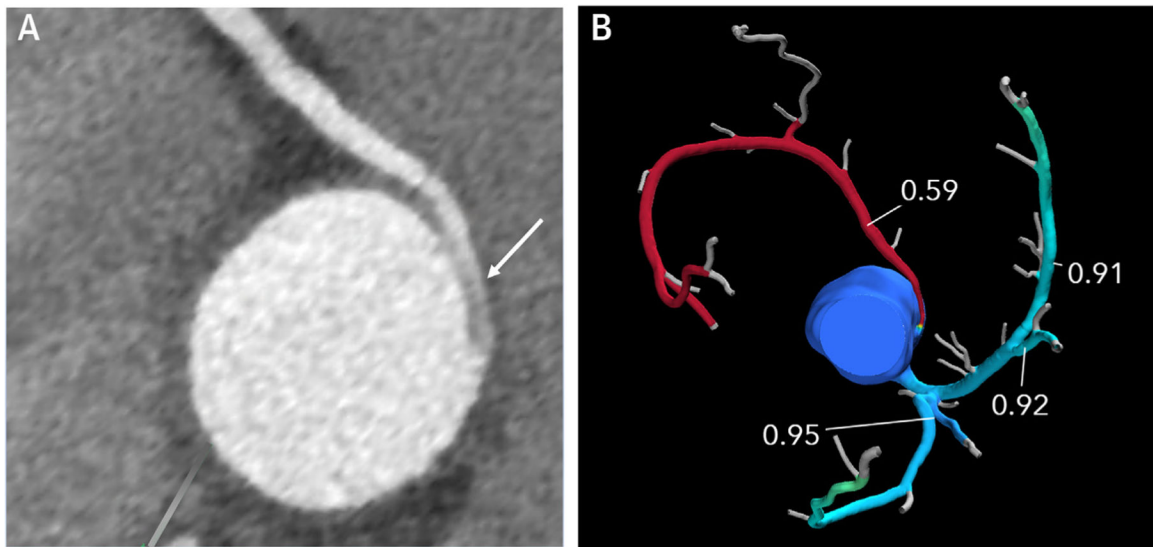


FIGURE 9. Computed Tomographic Fractional Flow Reserve (CT FFR)

(A) 2D short-axis CCT image of anomalous aortic origin of the right coronary artery from the ascending aorta just above the left sinus of Valsalva with an intramural proximal course (arrow) and normalization of vessel size as it leaves the aortic wall. The scan was performed using a dual source scanner with diastolic acquisition after administration of sublingual nitroglycerin. (B) CT FFR shows significant limitation to flow in the right coronary artery with a measurement of 0.59 at 2 cm distal to the anomalous origin.

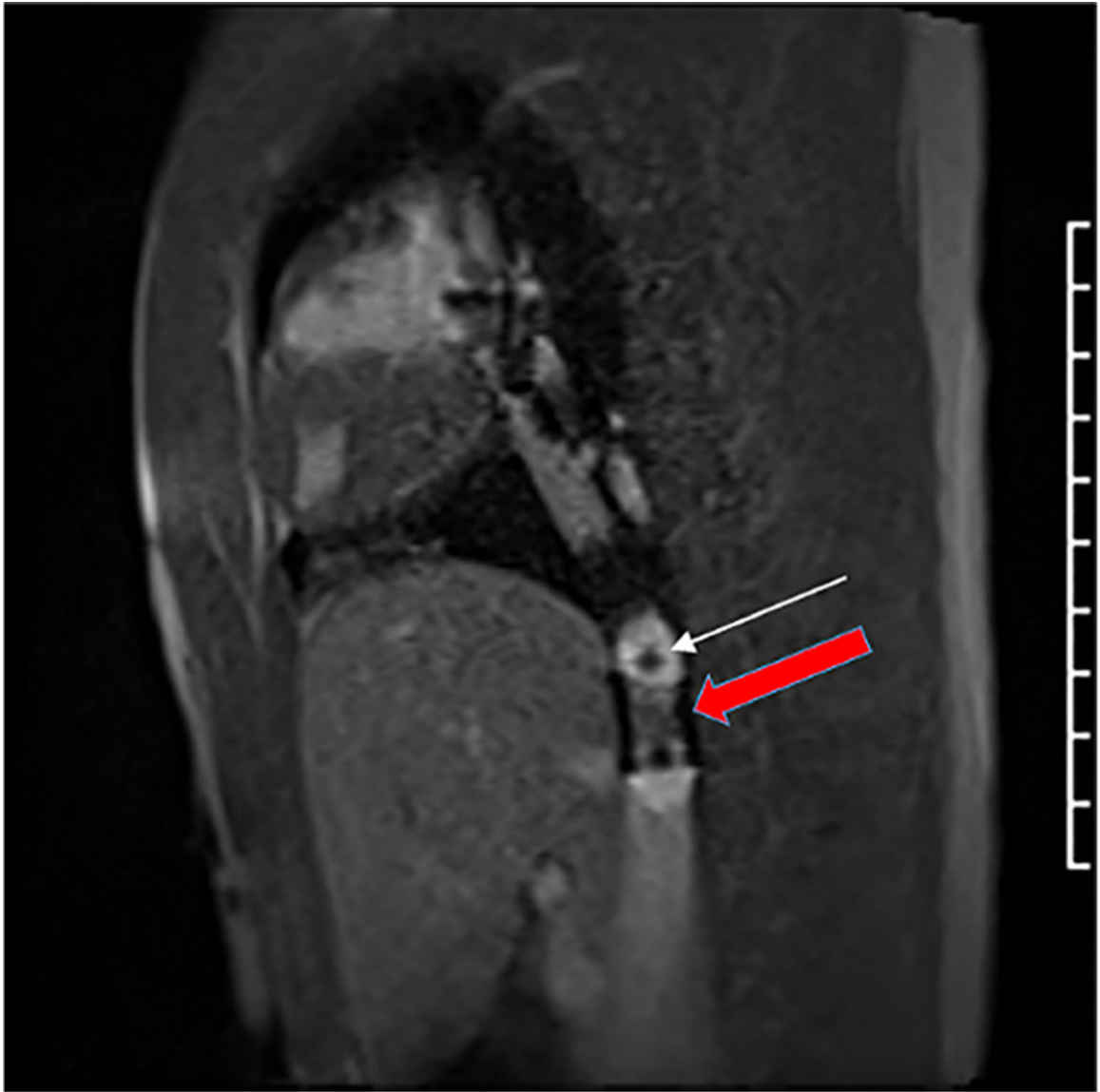


FIGURE 10. Interventional CMR Imaging

CMR still frame showing 20 mm × 3 cm balloon inflated with 1% gadolinium and 1 mm magnetic resonance–visible markers (white arrow) easily distinguished from the implanted stent (red arrow) in the inferior vena cava.

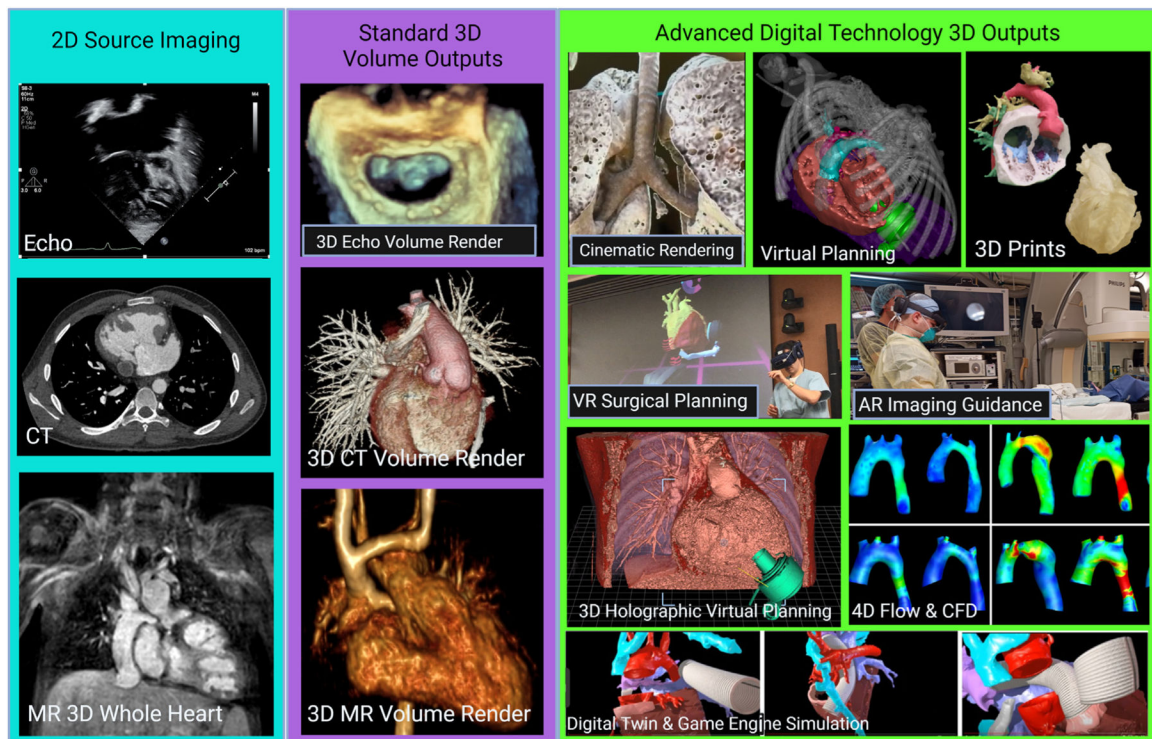



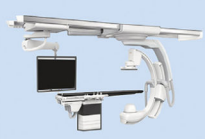
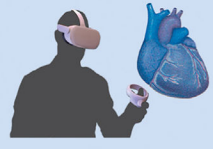


FIGURE 11. Advanced Digital Technology 3D Outputs in Congenital Heart Disease Imaging Reconstructed from stacks of 2D source data including echocardiographic (Echo), computed tomographic (CT), and cardiac magnetic resonance (MR) images (teal background), standard 3D volume outputs have become universally adopted for advanced 3D visualization in echocardiography, CT and MR (purple background). Exponential growth in higher quality and more interactive 3D outputs has created a wealth of new display options, including 3D printing to digital twin and virtual reality (VR)–based game engine simulation, particularly for hemodynamic predictions and procedural planning (green background). AR = augmented reality.

Clinical Applications of Congenital Cardiac Imaging Innovations

Echocardiography	Cardiac Magnetic Resonance	Cardiac Computed Tomography	Catheterization	Advanced Digital Technologies
 <p>3D Echo</p> <ul style="list-style-type: none"> • Valve morphology • Complex septal defects • Outflow tract obstruction • Complex intracardiac anatomy <p>Ultrafast Ultrasound</p> <ul style="list-style-type: none"> • Ventricular function • Vascular function • Myocardial and brain perfusion • Intracardiac flow dynamics 	 <p>3D Cine Imaging and 4D Flow</p> <ul style="list-style-type: none"> • Ventricular function • Vascular anatomy • Flow assessment in CHD <p>Tissue Characterization</p> <ul style="list-style-type: none"> • Myocardial scarring • Diffuse myocardial fibrosis • Myocardial edema <p>Lymphangiography</p> <ul style="list-style-type: none"> • Plastic bronchitis • Protein losing enteropathy • Chronic chylothorax • Chylous ascites 	 <p>Radiation Dose Optimization</p> <ul style="list-style-type: none"> • Patient specific scan protocol • ECG pulse modulation <p>Photon Counting</p> <ul style="list-style-type: none"> • Improved resolution • Spectral information • Decreased noise and metal artifact <p>Coronary FFR</p> <ul style="list-style-type: none"> • Coronary stenosis after reimplantation • Evaluation of anomalous coronaries 	 <p>3D Rotational Angiography</p> <ul style="list-style-type: none"> • Optimization of 2D gantry angles • Fusion with fluoroscopy • 3DRA-based CFD <p>Interventional Cardiac MR</p> <ul style="list-style-type: none"> • Low field scanning to visualize devices 	 <p>Extended Reality and Digital Twins</p> <ul style="list-style-type: none"> • Cardiac modeling • Complex intracardiac repair • Cavopulmonary connection • Vascular rings • Pulmonary artery reconstruction • Complex coronary cases • Virtual fit for mechanical circulatory devices • Transcatheter valve-in-stent

Artificial Intelligence

- Patient selection and protocoling, image acquisition, signal dosing, image registration and rendering, quantification, and interpretation

Sachdeva R, et al. *J Am Coll Cardiol.* 2024;83(1):63–81.

CENTRAL ILLUSTRATION. Innovations in Cardiac Imaging: A Novel Paradigm in CHD Evaluation

The novel imaging techniques in echocardiography (echo), cardiac magnetic resonance, cardiac computed tomography, catheterization, and advanced digital technologies have a broad range of clinical applications in congenital heart disease (CHD). In addition, artificial intelligence is being applied to different steps in the imaging process across all the cardiac imaging modalities. 3DRA = 3-dimensional rotational angiography; CFD = computational fluid dynamics; ECG = electrocardiogram; FFR = fractional flow reserve; MR = magnetic resonance.

TABLE 1
Novel Imaging Techniques in Congenital Heart Disease (CHD): Current Clinical Validation and Outcome Benefits

Imaging Technique	Validation	Outcome Benefits
3D echocardiography (3DE)	Validated in adults and CHD in small single-center studies	Accurate identification of orifices and borders, improved accuracy in diagnosis of valve abnormalities ⁵⁻⁸
Novel rendering techniques	Preliminary reports in pediatric CHD	Real-time 3DE guidance of transcatheter intervention, improved evaluation of valve pathology ³
Novel 3D transesophageal echocardiography probe	Research only	Not available
Ultrafast ultrasound	Research only	Not available
Ventricular and vascular function	Research only	Not available
Myocardial and brain perfusion	Early clinical use	Not available
Intracardiac flow dynamics		
Cardiac magnetic resonance imaging (CMR)		
Cine imaging and 4D flow	<ul style="list-style-type: none"> ● Good agreement with flow according to 2D phase-contrast measurements 	<ul style="list-style-type: none"> ● Comprehensive flow and shunts assessments in complex CHD²³ ● Flow characteristics and blood-tissue interactions may predict aortic dissection²¹ ● Quantification of atrioventricular valve regurgitation²²
Tissue characterization	<ul style="list-style-type: none"> ● Agreement with quantification of diffuse myocardial fibrosis on histology ● Correlation with systolic and diastolic dysfunction as well as adverse outcomes 	<ul style="list-style-type: none"> ● Markers of diffuse fibrosis as early indicators of myocardial remodeling²⁷ ● T1 tissue characterization is a confirmatory test for childhood myocarditis³⁷ ● Detection of heart transplant rejection³⁸
Lymphangiography	<ul style="list-style-type: none"> ● Findings complementary to those by fluoroscopic lymphangiography 	<ul style="list-style-type: none"> ● Greater lymphatic burden by T2 imaging is associated with adverse outcomes in single-ventricle patients, including Fontan failure⁴⁸
Cardiac computed tomography (CCT)	Accepted clinical practice	Decreased radiation dose for CCT ^{50,51}
Radiation dose optimization	Preliminary reports in CHD patients	Improved spatial resolution, lower radiation, metal artifact reduction ⁵⁷
Photon counting	Case reports only	May predict hemodynamic significance of AAOCA ^{60,61}
Coronary fractional flow reserve for anomalous aortic origin of a coronary artery (AAOCA)		
Catheterization		
Fusion imaging	Accepted clinical practice	<ul style="list-style-type: none"> ● Decrease in fluoroscopy time⁷⁴ and radiation exposure⁷⁵
3D rotational angiography	Accepted clinical practice	<ul style="list-style-type: none"> ● Decrease in radiation exposure⁶⁵ ● Improved diagnostic accuracy over 2D angiography⁶⁵
Interventional CMR	Preliminary reports in CHD patients	<ul style="list-style-type: none"> ● Decrease in radiation exposure^{77,79}
3D visualization		
3D printing	RCT in complex CHD, multiple case series in CHD, VAD, structural cardiac disease	<ul style="list-style-type: none"> ● Improved surgical approach in complex CHD⁹³ ● Improved visualization of deployed interventional devices⁹⁹

Imaging Technique	Validation	Outcome Benefits
Virtual procedural planning	Multiple case series and small single-center RCT	<ul style="list-style-type: none"> ● Improve device selection in catheter-based therapies⁹⁷ ● Improve surgical approach in CHD and other open heart surgical procedures^{101,102} ● Decrease planning time and increase accuracy⁹⁹

RCT = randomized controlled trial; VAD = ventricular assist device.